CHALMERS

Global response of ship hull during ramming of heavy ice features

Master's Thesis in the International Master's Programme of Naval Architecture and Ocean Engineering

MATHIAS BROMAN AND PER NORDQVIST

Department of Shipping and Marine Technology
Division of Marine Design, Research Group: Marine Structures
CHALMERS UNIVERSITY OF TECHNOLOGY
Göteborg, Sweden 2013
Master's Thesis X-13/290

MASTER'S THESIS IN THE INTERNATIONAL MASTER'S PROGRAMME IN NAVAL ARCHITECTURE AND OCEAN ENGINEERING

Global response of ship hull during ramming of heavy ice features

MATHIAS BROMAN AND PER NORDQVIST

Department of Shipping and Marine Technology
Division of Marine Design
Research Group Marine Structures
CHALMERS UNIVERSITY OF TECHNOLOGY

Göteborg, Sweden 2013

Global response of ship hull during ramming of heavy ice features
MATHIAS BROMAN AND PER NORDQVIST

Master's Thesis X-13/290
ISSN 1652-8557
Department of Shipping and Marine Technology
Division of Marine Design
Research Group: Marine Structures
Chalmers University of Technology
SE-412 96 Göteborg
Sweden
Telephone: + 46 (0)31-772 1000

Cover:
KV Svalbard during testing of the Ice Load Monitoring system in 2007, courtesy of Det Norske Veritas, Høvik.

Printed by Chalmers Reproservice
Göteborg, Sweden 2013

Global response of ship hull during ramming of heavy ice features

Master's Thesis in the International Master's Programme in Naval Architecture and Ocean Engineering

MATHIAS BROMAN AND PER NORDQVIST
Department of Shipping and Marine Technology
Division of Marine Design, Research Group Marine Structures
Chalmers University of Technology

ABSTRACT

The human presence in Arctic waters has increased and the development is assumed to continue. In order ensure that this increase in marine activities will be conducted in a safe manner, additional information about the factors that affect the marine structures in Arctic waters are required.

This master's thesis aims at analysing ice- induced global forces that affect a ship's hull when colliding with heavy ice features. This was done in order to increase the knowledge of what structural loads a ship encounters during Arctic operations and thereby contribute to a safer development in the Arctic. This was carried out by creating a model that used recorded motions of a ship when it collided with a heavy ice feature in order to calculate the global forces that affect the ship hull. The motion data was collected by Det Norske Veritas during the Coldtech research project on board the Norwegian Coast Guard vessel KV Svalbard.

To give an understanding and background to the problems that the model needs to handle, this thesis includes a brief review of sea ice properties and mechanics; ice class rules; and hull monitoring. These parts are used when the results are analysed and compared.

In addition, the model developed is limited to squared collisions and the first impact sequence, since only then the impact location can be considered known. Furthermore, it is also assumed that the ship can be seen as a rigid body; this is a normal assumption when dealing with ship motions.

The outcome of this study is a model that can be used for calculation of the ice-induced global forces that affect the ship's hull when colliding with a heavy ice feature. The results using the model are compared with the design load from ice class rules, since the same impact type is considered. The results are also compared with previous work done in the area. From the comparisons it can be seen that the forces calculated with the current model seem to be reasonable as they are in the same order of magnitude. However, more measurements are required in order to fully verify the model and the measured motions.

Key words: hull monitoring, hull motions, ice force, ice load monitoring, ice monitoring, ice-structure interaction.

Global respons på fartyg vid ramning av stora is-formationer
Examensarbete inom Naval Architecture and Ocean Engineering
MATHIAS BROMAN OCH PER NORDQVIST
Institutionen för sjöfart och marin teknik
Avdelningen för Marine Design, Forskargruppen Marine Structures
Chalmers tekniska högskola

SAMMANFATTNING

Närvaron i de arktiska farvattnen har under senaste åren ökat och denna utveckling förväntas fortsätta. För att kunna försäkra att denna ökade närvaro av marin aktivitet sker på ett säkert sätt krävs ytterligare information om de faktorer som påverkar marina strukturer i arktiskt klimat.

Detta examensarbete ämnar analysera de av havsis uppkomna globala krafter som påverkar ett fartygsskrov vid kollision med stora isformationer. Detta för att utöka kunskapen kring de laster en fartygsstruktur möter under segling i arktiska farvatten och därmed bidra till en säkrare utveckling i Arktis. Detta har gjorts genom att skapa en modell som använder uppmätt data av ett fartygs rörelser vid kollision med stora isformationer för att beräkna de globala krafter som verkar på fartygets skrov. Data innehållande fartygets rörelser har samlats in av Det Norske Veritas under Coldtech, ett forskningsprojekt ombord den norska kustbevakningens fartyg KV Svalbard.

För att ge förståelse och god bakgrund till de problem modellen hanterar, inkluderar examensarbetet även en kort sammanfattning av havsisens egenskaper och mekanik, isklassregler samt fartygsövervakningsmetoder. Dessa delar används när resultaten analyseras och jämförs.

Modellen som utvecklats är begränsad till att enbart utvärdera kollisioner där fartyget träffat isen i rät vinkel och enbart den första kollisionssekvensen. Detta då enbart under dessa förhållanden kan det anses att positionen där den resulterande kraften verkar är känd. Vidare är det antaget att fartyget kan ses som en stel kropp, detta är ett vanligt antagande när fartygsrörelser utvärderas.

Resultatet av studien är en modell som beräknar de av is uppkomna krafterna som verkar på fartygets skrov under kollision med stora isformationer. Modellens resultat jämförs med den dimensionerande kraften från isklassregler då dessa bygger på samma typ av kollision. Resultaten jämförs även med resultat från liknande studier. Från dessa jämförelser kan det dras slutsatsen att de med modellen beräknade krafterna är rimliga i sin storlek. Mer mätningar krävs för att till fullo kunna utvärdera och verifiera både modellen och de uppmätta rörelserna.

Nyckelord: fartygsrörelser, fartygsövervakning, iskraft, islastövervakning, is-struktur interaktion, isövervakning.

Contents

Preface

This thesis is a part of the requirements for the master's degree in Naval Architecture and Ocean Engineering at Chalmers University of Technology, Göteborg, and has been carried out at the Division of Marine Design, Department of Shipping and Marine Technology, Chalmers University of Technology in cooperation with Det Norske Veritas, Division of Maritime Advisory in Høvik, Norway, between January and June of 2013.

We would like to acknowledge and thank our examiner and supervisor, Professor Jonas Ringsberg at the Department of Shipping and Marine Technology for his excellent guidance and support throughout the work with this thesis. Furthermore, we would also like to thank our main industry supervisor Håvard Nysedth at the Section of Ship Structure and Concepts at Det Norske Veritas in Høvik, Norway, for his time and excellent guidance, especially in the field of ice-structure interaction.

Finally we would like to thank our co-supervisors, Maura Rowell, Visiting Researcher at the Department of Shipping and Marine Technology, and Alessio Prestileo at Det Norske Veritas, for their time and help, as well as Morten A. Lerø, Head of Section Ship Structures and Concepts at Det Norske Veritas for giving us the opportunity to perform this master's thesis.

Göteborg, June, 2013

Mathias Broman and Per Nordqvist

Notations

Abbrevations

ABS	American Bureau of Shipping
Acc.	Acceleration
Disp.	Displacement
DNV	Det Norske Veritas
DOF	Degrees of Freedom
IACS	International Association of Classification Societies
ILM	Ice Load Monitoring
LNG	Liquefied Natural Gas
MOTAN	Motion Analysis System
MRU	Motion Reference Unit
NASA	National Aeronautics and Space Administration
NSR	Northern Sea Route
Vel.	Velocity

Ship-based coordinate system

x-axis	Horizontal axis along the length of the ship with zero at the centre of gravity, positive towards the bow.
y-axis	Horizontal axis along the beam of the ship with zero at the centre of gravity, positive to port.
z-axis	Vertical axis with zero at the centre of gravity, positive upwards.

Ship motions

Heave	Translational motion along the z-axis, positive upwards.
Pitch	Rotational motion about the y-axis, positive with bow moving downwards.
Roll	Rotational motion about the x-axis, positive with port side moving downwards.
Surge	Translational motion along the x-axis, positive forward.
Sway	Translational motion along the y-axis, positive to port.
Yaw	Rotational motion about the z-axis, positive with bow moving port.

Roman upper case letters

A	Added mass matrix (6×6)
	$[\,ton\,]$ (column 1-3, row 1-3)
	$[\,ton\cdot m\,]$ (column 1-3, row 4-6)
	$[\,ton\cdot m\,]$ (column 4-6, row 1-3)
	$[\,ton\cdot m^2\,]$ (column 4-6, row 4-6)
B	Hydrodynamic damping matrix (6×6)
	$[\,ton/s\,]$ (column 1-3, row 1-3)
	$[\,(ton\cdot m)/s\,]$ (column 1-3, row 4-6)
	$[\,(ton\cdot m)/s\,]$ (column 4-6, row 1-3)
	$[\,(ton\cdot m^2)/s\,]$ (column 4-6, row 4-6)
C	Hydrodynamic stiffness matrix (6×6)
	$[\,ton/s^2\,]$ (column 1-3, row 1-3)
	$[\,(ton\cdot m)/s^2\,]$ (column 1-3, row 4-6)
	$[\,(ton\cdot m)/s^2\,]$ (column 4-6, row 1-3)
	$[\,(ton\cdot m^2)/s^2\,]$ (column 4-6, row 4-6)
F	Force vector (6×1)
	$[\,N\,]$ (column 1-3)
	$[\,Nm\,]$ (column 4-6)
M	Ship mass matrix (6×6)
	$[\,ton\,]$ (column 1-3, row 1-3)
	$[\,ton\cdot m\,]$ (column 1-3, row 4-6)
	$[\,ton\cdot m\,]$ (column 4-6, row 1-3)
	$[\,ton\cdot m^2\,]$ (column 4-6, row 4-6)

Roman lower case letters

x	Distance in the x-direction
y	Distance in the y-direction
z	Distance in the z-direction

Greek lower case letters

η	Position/Displacement-vector (6×1) $[m]$ (column 1-3) $[rad]$ (column 4-6)
$\dot{\eta}$	Velocity-vector (6×1) $[m/s]$ (column 1-3) $[rad/s]$ (column 4-6)
$\ddot{\eta}$	Acceleration vector (6×1) $[m/s^2]$ (column 1-3) $[rad/s^2]$ (column 4-6)

Subscript

1	In the x-direction
2	In the y-direction
3	In the z-direction
4	Rotational direction about the x-axis
5	Rotational direction about the y-axis
6	Rotational direction about the z-axis
B	Due to hydrodynamic damping
C	Due to hydrodynamic stiffness
COG	At the centre of gravity
E	External
MRU	At MRU position
R	Reaction

1 Introduction

This chapter starts with a brief background to the thesis. It is followed by the objective, methodology, limitations and the outline of the thesis.

1.1 Background and motivation of work

Over the past decades, especially the last few years, the interest in human presence in the Arctic area has increased dramatically. This increased presence has its source in a number of reasons, mostly related to climate and the market.

In September 2012, NASA reported that the Arctic ice cover has reached its lowest point in the satellite era. Figure 1.1 shows the sea minimum ice extent in 2012 (the white area) compared with the average minimum extent over the last 30 years (the solid line), NASA (2012). The figure shows that the minimum sea ice extent in 2012 is much less than the average minimum sea ice extent. This can be connected with reports that state that the earth's mean temperature has increased over time. This is considered to be an effect of the increased amount of carbon dioxide and other greenhouse gases in the atmosphere, IPCC (2007). The mean temperature is rising at its fastest in the Arctic area, and the continuous increase of carbon dioxide in the atmosphere makes research efforts to point towards a continuous increase of the earth's mean temperature, which will affect the melting of the polar ice cover and probably cause it to further decrease, IPCC (2007).

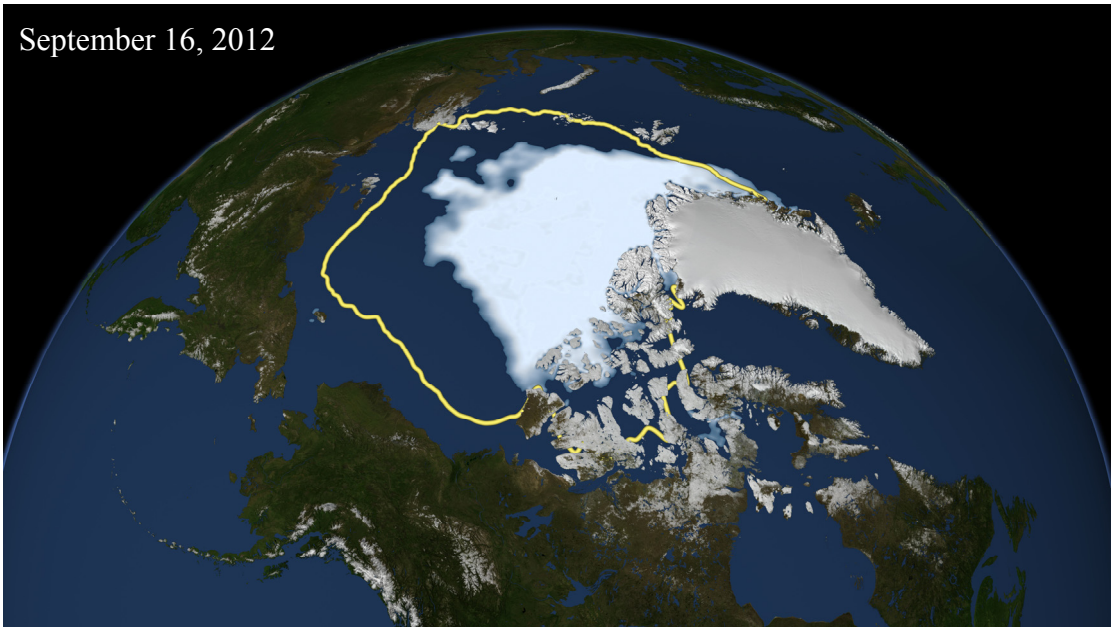

Figure 1.1 Minimum Arctic sea ice extent 2012 (white area) compared with the average minimum extent over the last 30 years (solid line), NASA (2012).

The shrinking ice covers increases the possibility of using the Northern Sea Route, NSR, when transiting from Asia to Europe. The NSR goes north from South East Asia through Bering Strait and onwards to Murmansk in Russia, and Europe (see the dashed line in Figure 1.2, the NSR, compared with the solid line, the traditional

trading route through the Suez-canal). The NSR is currently being used to a minor extent, mainly to transport raw materials and LNG from Norway and Russia to China and Japan. The trend is an increased use of the NSR, with 4 voyages in 2010, 34 in 2011 and 46 in 2012, Pettersen (2012). The sea distance decreases by about half from Hammerfest in Norway to Shanghai and by about one third from Rotterdam to Shanghai compared with the regular route through the Suez Canal. In addition to the shorter voyage, the NSR avoids the risk of piracy around the Horn of Africa, which has been a concern during the past few years, Blunden (2012).

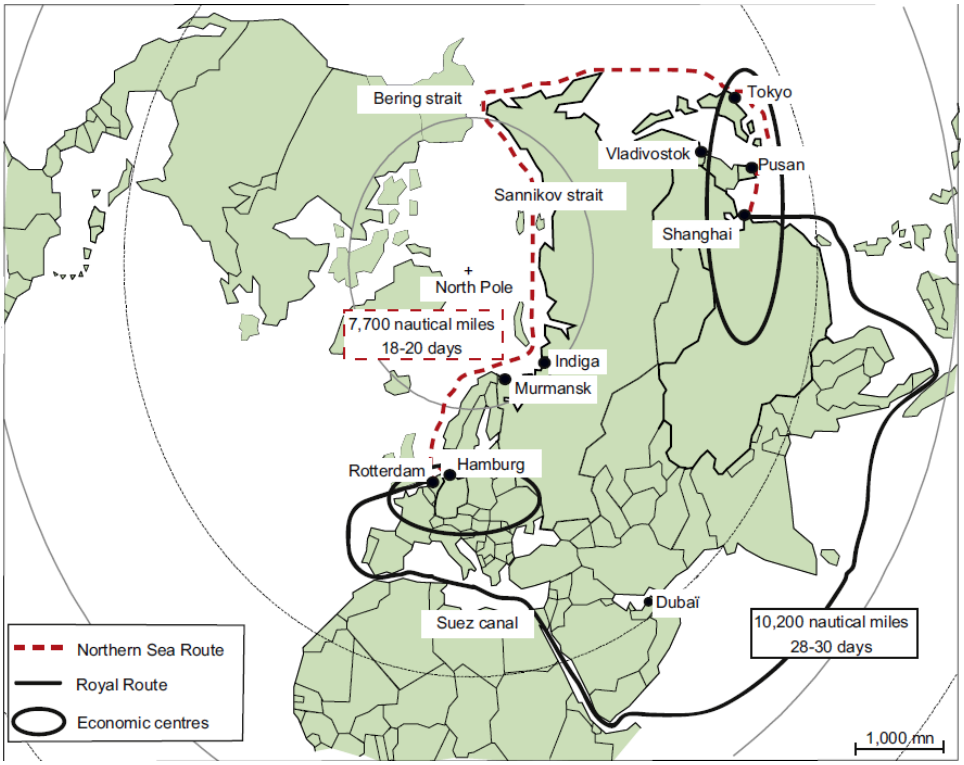

Figure 1.2 *Nothern Sea Route (dashed line) compared with regular trading route through Suez-canal (solid line), Verny and Grigentin (2009).*

Increased prices on oil, gas and minerals bring another type of interest into the Arctic area. It is estimated that up to 13 per cent of the remaining undiscovered oil and 30 per cent of the remaining undiscovered natural gas lies within the Nordic Arctic Circle, USGS (2008). With an easier access to the resources due to climate changes, a rapid increase of oil, gas and mineral exploration is expected in the near future.

There are several factors that drive the exploitation of the Arctic waters, and this trend will most probably continue in the near future. However, the melting of the ice cover will not erase the risks of marine operations in a cold climate. In March, when the ice cover is at its largest, the ice will still cover the whole area within the polar circle with the exception of the area between the northwest coast of the Scandinavian Peninsula and Greenland, which is kept ice-free by the Gulf Stream, IPCC (2007).

When the polar sea ice is melting, the melting process will cause strains and cracks through the ice cover. This, in combination with the year-round dynamic motions of the ice cover, which is driven by wind, currents etc., will eventually cause chunks of ice to break away and form large ice floes. The ice floes may drift into offshore

structures or collide with ships. An increased temperature will cause the large glaciers to melt faster, which gives more and larger icebergs when the glacier calves. Hence, the warming will affect the ice condition in Arctic waters in different ways. The large glaciers on Greenland will calve more, thereby creating more icebergs that will drift south with the Labrador Current along the North American coast. If larger icebergs are created when the glacier calves it means that the icebergs will travel further south before they melt and this will affect the transatlantic trade, Lundhaug (2002). Global warming does not only give a smaller ice extent in the Arctic waters; in the Antarctic, the sea ice is extending. This is, according to Bintanja et al. (2013), due to the cold melt water from Antarctic shelves accumulating in a cold surface layer that enables the sea ice cover to grow. This means that challenges due to sea ice arise all the year round, with continuous ice, cold weather and Arctic storms in the winter and the risk of encountering occasional ice features like large floes, growlers and icebergs in the summer.

If the implication of sea ice interference with marine structures is not sufficiently investigated, the consequences that might follow could be dire. Obviously, this involves the economic loss of marine units that are in operation, but, more importantly, rescue operations will be severely impaired by the cold and the ice, giving longer response times during, for example, an oil spill. The environment in the Arctic area is sensitive; long response times and the consequences due to limited possibilities of containing an oil spill beneath the ice must not be overlooked, USARC (2012).

As the difficulties with marine operations are well known to all parties involved, the extent of research within the field has increased; this is to allow the presence in the Artic area to be conducted in a safe manner with limited consequences of any accidents. The research efforts consider the whole spectrum from structure-ice interaction to emergency responses in case of an incident. Although transiting ice-infested waters is nothing new, the structural response from ice loads is poorly understood due to the random characteristics of the loads and is still in need of much investigation, Mejlaender-Larsen and Nyseth (2007).

In the research project, Coldtech Nyseth et al. (2013), managed by DNV and supported by the Norwegian Research Council, measurements of ice response on the coast guard vessel KV Svalbard were performed. The goal was to increase the overall understanding of the actual ice condition that the vessel encounters. During the measurements in 2007, strain-sensors were applied to the bow to record the response of ice impact. As an extension to the project, an additional set of measurement equipment was installed on KV Svalbard in 2011 and 2012 in order to measure the global motions of an ice impact. The motions can be used for several purposes; as a design parameter for cargo securing; for manoeuvring feedback; for investigating the working conditions of the crew. It can also be used for analysing the ice- induced global forces that created the structural response, DNV (2009).

1.2 Objective

The objective of this master's thesis is to create a model that calculates the ice-induced global forces on a ship's hull based on measured global motions of a ship that travels in ice-infested waters and collides with an ice-feature. This model should be used for giving quantified data about ice-induced global forces and ship-ice

interaction when ice class rules are developed. This is possible, since the model is developed for the same type of impact as the dimensioning load case in the class rules. An increased knowledge in the types of loads that a ship travelling in Arctic regions encounters will make the development of increasing traffic in Arctic regions safer, as described in Chapter 1.1. This opens up the possibility of both a more sustainable transportation of cargo as the route distance may decrease as well as create less hazardous solutions of exploiting the natural resources.

1.3 Methodology

The methodology of this thesis is presented in Figure 1.3. The motion data have been collected by DNV during the Coldtech research project on the Norwegian coastguard vessel KV Svalbard as described in Chapter 1.1. The data from these measurements have been post-processed by analysis of the frequencies of recorded motions. Different motions have different frequencies, and only the motions with same the frequency as ice- induced motions have been kept. Subsequently, the impact events have been identified, and motions at relevant impacts were used to calculate the ice-induced global force by using the equation of motion. Post-processing of data and force calculations were performed in MATLAB software, MathWorks (2011). Finally, the results have been evaluated, the validity of the results examined and then compared with similar work done, i.e. Johnston et al. (2001) and Johnston et al. (2003).

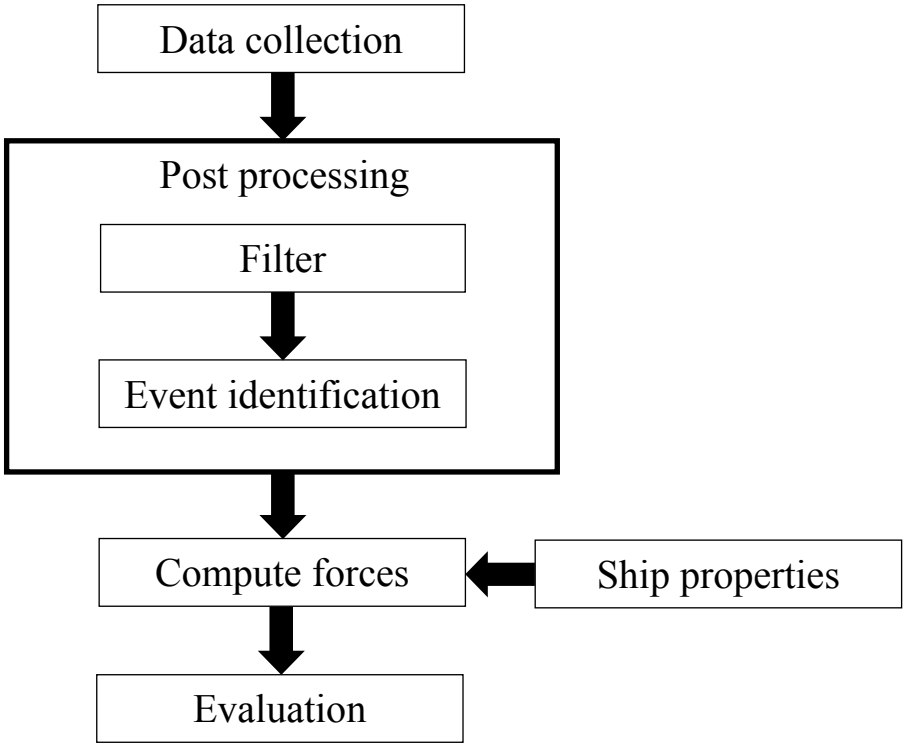

Figure 1.3 Methodology of the thesis.

1.4 Limitations

The data analysed in this work only consisted of measurements from a motion reference unit, MRU, on board KV Svalbard during the Coldtech research project. The impact intervals that were evaluated were defined beforehand and can be found in

Nyseth (2012). This means that this model needs a time stamp where any supposed impact has taken place, either automatically or manually. In this case the time for impacts was manually inputted.

In the ship motions analyses it was assumed that the ship behaved like a rigid body, which is a normal assumption when dealing with ship motions. One should, however, be aware of the effect of this assumption. When a ship responds to an external force, the response can be divided into an elastic body response and a rigid body response. This assumption means that we are neglecting the energy from the collision that will be dissipated through the elastic body response, and the resulting forces will therefore be on the lower side. The assumption can be made with the motivation that KV Svalbard has a high ice class, which means that it is a rigid construction that allows only for small elastic deformations.

It was assumed that the ship hit the ice edge with a square angle from open water. This assumption gave the position of the impact on the hull, and the impact could be assumed to act at the bow in the water plane. This affected the results if the impact was not squared, as some of the computations presumed that the levers from the ice impact to centre of gravity were known.

Only the first response period after the impact was considered, as the position of the force became more uncertain as the bow penetrated the ice. This means that the lever from the ice force to the centre of gravity will be considered as being known during the whole impact period.

1.5 Outline of thesis

To provide more background to the complexity of the load case, a brief summary of sea ice properties and mechanics are presented in Chapter 2. Chapter 3 briefly describes ice class rules, with a focus on the IACS polar class, as the polar class rules are based on a load case similar to the load case in this study. This is followed by examples on hull monitoring systems, with a focus on ice- load monitoring in Chapter 4. Here, a summary of the equipment on board KV Svalbard is given together with a description of similar research projects. The computational model developed in this thesis is presented in the Chapter 5. The results achieved in the study are presented and discussed in Chapter 6, followed by conclusions in Chapter 7 and recommendations for future work in Chapter 8.

2 Sea ice

In order to make sure that the correct assumptions for the developed model are made it is necessary to understand how sea ice is shaped, what properties it has and how these properties come into play when the ship is ramming ice. This chapter aims at providing the necessary context in order to comprehend the limitations of the model presented in this thesis. This chapter includes a brief presentation of variable influences of the shaping of sea ice that affects the properties followed by a description of how different failure modes and the different load cases this creates. This chapter includes a short description of the ice-structure interaction followed by external mechanics of ice-ship collision to provide an understanding of how the motion response of the ship may look and to be a part of the evaluation of the result.

2.1 Environmental influences of sea ice

Sea ice is a wide expression. It includes shapes from recently formed crystals that are weakly frozen together to multi-year ice that has survived for several melting seasons. This chapter aims, in a brief way, at describing why sea ice properties vary in order to assess the validity of the work. For a more thorough description of sea ice development, physical and mechanical properties, see WMO (2004), Timco and Weeks (2010), and Bureau Veritas (2010).

Various impurities with varying concentrations are included in the ice as a consequence of different environmental influences. This causes the properties of the sea ice to vary. The main factors that the properties of sea ice depend on are, according to Timco and Weeks (2010) and Bureau Veritas (2010):

- Temperature of ambient air and water
- Freezing time
- Wind speed
- Thickness of snow cover
- Microstructure
- Grain size
- Salinity and brine volume
- Porosity
- Ice type
- Formation of the ice
- Loading direction
- Loading rate

Ambient temperature, freezing time, wind speed and the thickness of the snow cover affect the formation and growth of the ice. This is crucial since the thickness and development stage of the ice are two of the most important parameters when analysing ice-structure interaction. The surrounding environment when sea ice forms affects the microstructure and grain size of the sea ice. There are two microstructure types that can be formed, namely granular and columnar. Granular microstructure usually generates an isotropic material and has smaller grains than columnar microstructure. Columnar microstructure can generate an anisotropic ice structure with very large grains. Sea ice is formed by sea water which consists of salt in various concentrations. When sea water freezes most of the salt will be drained from the ice crystals, but some salt is enclosed either as salt crystals or as liquid brine. Since brine has a lower freezing point than water it slowly melts its way downwards through the ice and thereby causes older sea ice to be more porous and has a lower degree of salinity and density than younger sea ice. Even though sea ice exists close to its melting point it can for loading rates experienced in engineering practice be seen as a brittle material, Timco and Weeks (2010), and Bureau Veritas (2010).

2.2 Failure of ice

The brittle characteristics of sea ice result in a non-simultaneous failure along the contact zone between ice and ship. The non-simultaneous failure gives a non-uniform pressure distribution over the contact zone. The peak pressure gets higher, which results in an even more brittle behaviour, Bureau Veritas (2010).

When sea ice fractures due to collision against some geometry, there is often failure in several ways simultaneously. This can be seen in Figure 2.1 below where there is failure by crushing; where fracture causes small pieces of ice to spall off, near the structure; and failure due to bending some distance in front of the structure, Jordaan (2001).

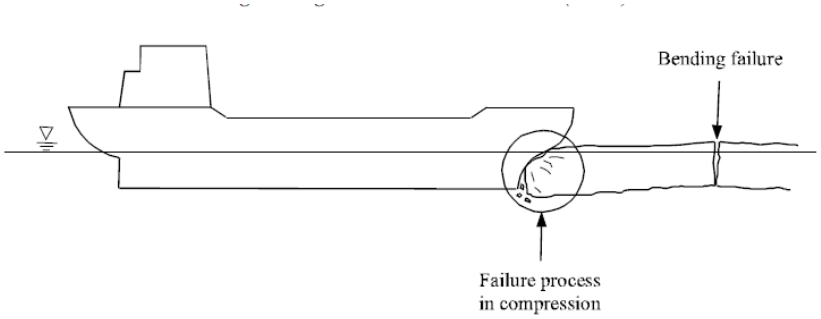

Figure 2.1 Ship ramming into an ice floe with crushing failure close to the bow, and bending failure at some distance forward of the ship, Jordaan (2001).

Ice has a different strength against the different failure modes buckling, crushing and bending. The limit between buckling and bending are dependent on the inclination angle and the friction between the ice and the structure. For an event occurring in engineering practice, ice fails in bending rather than in buckling, Bureau Veritas (2010).

The limit between bending and crushing failure of the ice is dependent on the impact area. A small impact area gives failure by crushing and a larger area gives failure by bending. But because of the irregular brittle failure of an ice feature against a structure there will always be some extent of crushing together with bending failure of the ice. This means that the failure mode that affects the global forces on a ship are governed by the fact that bending failure and crushing failure will contribute to the local forces and is thereby the cause of local high-pressure zones on the hull, Bureau Veritas (2010).

2.3 Ice-ship interaction

Computing ice loads is a challenge because of varying ice conditions and the complicated nature of ice-structure interaction. Ice forces affect a ship's hull both locally and globally. The global loads can generate bending in the hull girders and, through this, affect the global structure of the ship, while the local ice forces affect the local structure. There is a large variation of pressure across a compressive interface between ice and a structure. The loads are transmitted through a number of zones where a high pressure is received. These zones can be considered as point loads and vary over the interaction surface, Jordaan (2001).

Because of the random behaviour of sea ice failure, there is no way to predict the exact local force on a certain point of a structure interacting with ice. However, there exists ways to estimate local forces by measuring the pressure on the ship's hull when breaking ice. These measurements can give a pressure distribution where a high pressure zone has a certain probability to occur at different points. By using this distribution and either calculating or measuring the global forces, the local pressure can be estimated, Jordaan (2001), and Croasdale and Frederking (1986).

According to Daley and Riska (1995), Bureau Veritas (2010), Suyuthi et al. (2012) and Suyuthi et al. (2011), when the hull first comes into contact with the ice, the ice will be crushed and spall will be created until the contact force becomes large enough for flexural failure, tipping and clearance of ice. This behaviour creates a saw-tooth shaped force plot over time. The force increases from initial crushing until breaking, after which the force drops until the next encounter where the series starts again. These forces will cause a pitching and heaving motion as the resulting force will be upwards as the ship penetrates the ice. In addition to this the ship will lose speed, which is the surging motion. When the ice fails due to bending, the heave and pitch will proceed downwards. The random characteristics of ice failure may or may not cause roll, sway and yaw motions when breaking ice. As the failure of ice is hard to predict, it is hard to decide what the load case will look like. There are several empirical methods for calculating the resulting ice force see Bureau Veritas (2010) and Suyuthi et al. (2011).

2.4 External mechanics in a ship-ice collision

The analysis of a collision between a ship and an ice-feature is complex; for simplification it is often divided in two parts, Liu (2011):

- External mechanics: Determine the energy to be dissipated as strain energy.
- Internal mechanics: Determine how the strain energy is dissipated within the two bodies.

Before impact, both the ship and the ice feature have a kinetic energy, but the relative velocity is often largely governed by the ship's speed. When the ship and an ice feature collide, some of the initial kinetic energy is dissipated through the deformation of the bodies and some energy remains as kinetic energy of the ship and iceberg after a collision. The main factors that determine how much of the initial kinetic energy is to be dissipated as strain energy are the masses of the ship and iceberg and the relative velocity between them, Popov (1967) and Liu (2011).

There are several methods for calculating the dissipated energy. One of the first to develop a model for ice impacts was Popov (1967). He approached the problem by assuming that kinetic energy in the impact direction is dissipated as strain energy in the bodies. Another more recent approach was developed by Liu (2011). By using the coefficient of restitution he calculated the difference in kinetic energy before and after a collision and thereby the dissipated energy in all three directions.

There are several strategies for determining what body it is that dissipates the strain energy. Three main strategies can be distinguished:

- Ductile design
- Shared energy design
- Strength design

In ductile design, the iceberg can be seen as a rigid body and the ship has to absorb all the strain energy dissipated. Since the ship structure is well known this strategy simplifies the analysis, but high demands are set on the ship's strength. In strength design the ship crushes the ice with minor structural deformation. The structure must thereby resist the maximum pressure that the ice applies on the contact area. Shared energy design is something inbetween; it implies that both bodies absorb dissipated energy and deformation. Generally, the stronger of the two bodies absorbs less energy, but the relative strength varies during the impact and therefore this strategy is complex (see Figure 2.2a). The relation between impact force, deformation and dissipated energy can be seen in Figure 2.2b. The dissipated energy is the area under the force-deformation curve, Liu (2011).

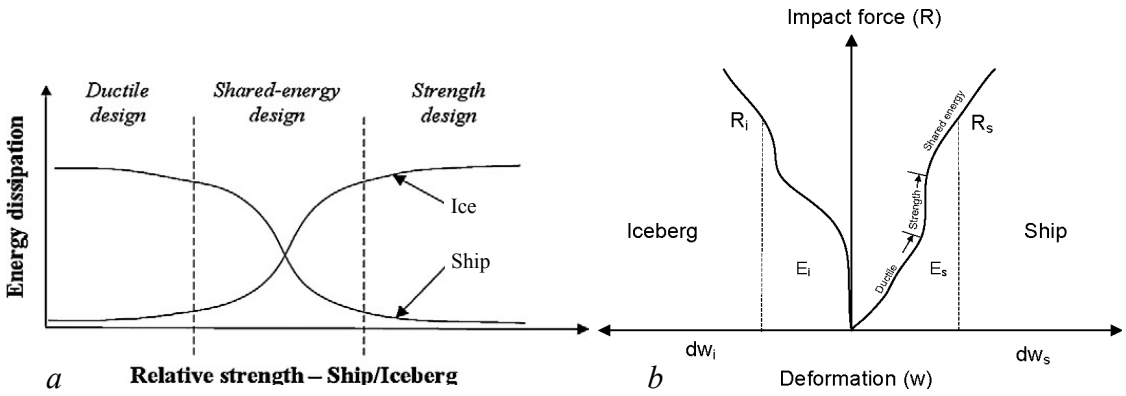

Figure 2.2 Energy dissipation in ductile, shared energy and strength design in a) and energy dissipation as a function of impact force and deformation in b), Liu (2011).

3 Ice Class Rules

Sea ice causes additional loads cases that are hard to predict. However, in order to create design rules for a ship to travel in ice infested waters, some rational approach is needed. The ice class rules have traditionally been based on previous accidents and incidents where each cause of failure was investigated and used for improving the safety of a vessel operating in Arctic conditions. This has created a number of empirical and semi-empirical formulas to decide the design parameters. In the latter part of the 20th century, a more proactive approach was taken, where the design loads were based more upon theory and calculations of the ship's structural strength. In this approach it is necessary to have measurements for relating to and verifying the dimensional loads used for the calculations. This chapter briefly describes how the International Association of Classification Societies' (IACS) unified ice class rules are built up; what scenario defines the load case that causes the dimensioning load and how this thesis work fit into the ambition to improve the ice class rules.

3.1 Polar Class notation

There are several different notations for ice class rules as the class societies have their own notations. Since 2007, however, when IACS released their Unified Requirements for ice classification (IACS UR I1, I2 and I3) there is one common set of rules intended for ships that are operating in ice-infested waters. These requirements are additional to the open-water requirements for each member society. The requirements divide the polar class into seven notations from PC1 to PC7, see Table 3.1, IACS (2010) and DNV (2012).

Table 3.1 Polar class notations from DNV (2012) and IACS (2010).

Polar Class	Ice Description (based on WMO Sea Ice Nomenclature)
PC 1	Year-round operation in all Polar Waters.
PC 2	Year-round operation in moderate multi-year ice conditions.
PC 3	Year-round operation in second-year ice which may include multi-year inclusions.
PC 4	Year-round operation in thick first-year ice which may include old ice inclusions.
PC 5	Year-round operation in medium first-year ice which may include old ice inclusions.
PC 6	Summer/autumn operation in medium first-year ice which may include old ice inclusions.
PC 7	Summer/autumn operation in thin first-year ice which may include old ice inclusions.

The notation PC does not include icebreakers, which, on top of conditions described in Table 3.1, should be designed to operate independently. Specific regulations for each classification society hold in this case. The hull requirements are based on a scenario with a collision between a ship and an ice feature called a glancing impact, which is a single hit at the forward part of the ship. This type of hit is similar to the impacts that were investigated during this thesis work. The impact results in a force that acts on the hull and the magnitude of the force is dependent on the current ice conditions. As the different Polar Classes allow different types of ice encountering, the design force will be different for each ice class. This means that the maximum strength and resistance for a single impact is a design factor for a ship operating in polar waters, DNV (2012). As the hits studied in this thesis work involved heavy ice features, such as ice ridges and growlers, the related polar class was chosen to be PC 1. The design load as given by PC 1 was used for comparison with the load case in this thesis, see Chapter 6.2.

The ship's hull is divided into different areas, see Figure 3.1 below. These regions get different ice load factors and are thereby designed for different loads. The resistance for each area is designed with an allowance for deformation.

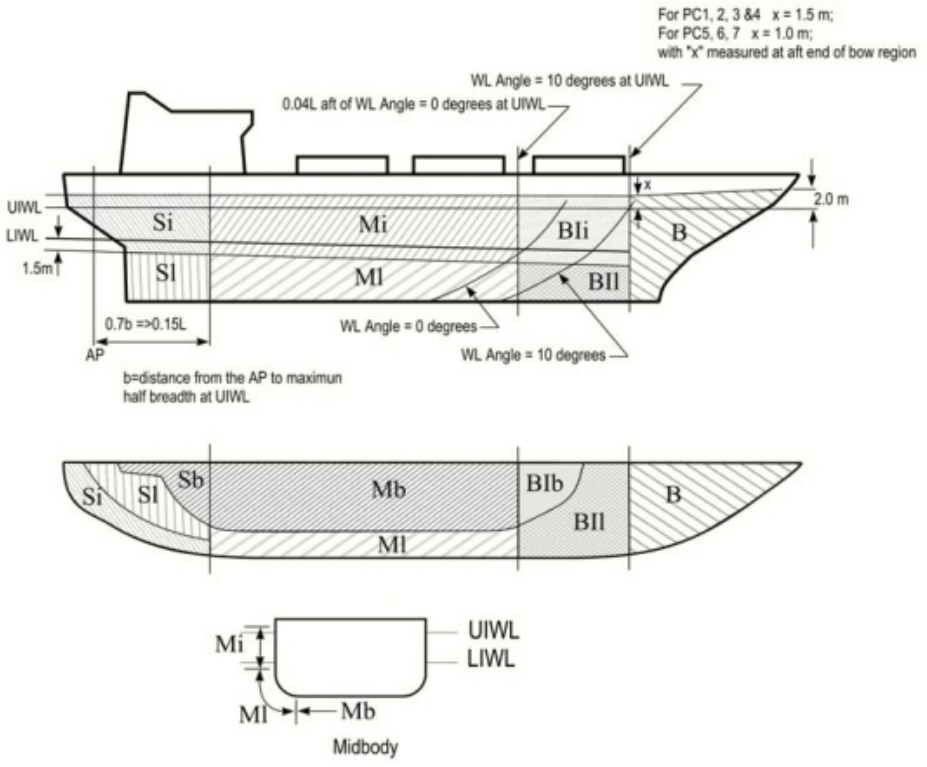

Figure 3.1 Description of hull areas according to DNV (2012) and IACS (2010).

3.2 Limit state design

Traditionally, rules have been based on an allowable stress design where the design aims at keeping the stresses from a design load under a certain working stress, but this is according to IACS (2009), which is a guideline intended to be used so that new structural rules apply with IMO's Goal-Based New Ship Construction Standards, IMO

(2011), “The rules are to be based on the principles of limit state design”. Limit state design is in contrast to allowable stress design based on various conditions where the structure needs to fulfill its intended function. Four limit states are relevant for marine structures:

- Serviceability limit state (SLS)
- Ultimate limit state (ULS)
- Fatigue limit state (FLS)
- Accidental limit state (ALS)

Serviceability limit state concerns functionality during operational conditions, ultimate strength concerns extreme loads and the ultimate strength of the structure. Fatigue limit state concerns long-term usage during operational conditions, and accidental strength concerns less common situations with abnormal loads, IACS (2009).

Accidental limit state design mainly aims at avoiding loss of life, avoiding pollution and minimizing loss of property in case of an accidental event. The main safety functions of the structure must remain after the accidental event. Typical accidental events can be grounding, collision with a ship or iceberg, or internal explosions. Accidental limit state design can be described by the reasoning in Chapter 2.5. All dissipated energy can be assumed to go into the ship, which means that the ship is designed according to ductile design, IACS (2009).

Ultimate limit state design is based on the ultimate strength of the structure - the point where plastic collapse of the structure occurs. The ultimate strength of the structure is estimated or calculated and the structure is subsequently designed with a safety margin. Referring back to Chapter 2.5, this is if the safety margin makes the design shift from ductile to strength design. A small safety margin gives ductile design and a larger safety factor gives strength design, IACS (2009).

In the case of ice class rules, they are based on ALS and ULS events, since they consider an extreme event as a design event. However, rules are mostly based on previous knowledge and analyses of old design in contrast to ALS and ULS which are based on a design load with a return period of 20-30 years, which is the expected lifetime of the ship. These design loads allow for minor permanent deformation on the ship structure, IACS (2009).

4 Hull monitoring

As the transition towards a more theoretical basis for the classification rules is made, the need to verify both the computation and the assumed load cases arises. It is also important to make sure that the ship operates within the limitation of the vessel's class notation. To aid this, a hull-monitoring system can be installed on the vessel. This chapter provides a brief background on some of the different general hull-monitoring possibilities and how they can be applied to measure ice loads. A brief introduction to a study that is similar to the one presented in this thesis is also presented as well as a description of the hull-monitoring equipment on KV Svalbard.

4.1 Applicability

The applicability of hull-monitoring systems stretches over a large variety of incidents. A few examples are: strain gauges in order to measure, for example, plate loading or hull girder stresses; installing accelerometers to assess motion sickness index, risk of cargo damage or risk for slamming incidents; and measuring the current fuel consumption and engine output. The hull-monitoring system can be applied either as an aid for the crew aboard the ship in order to make the best navigational decisions at each instant or as a way of collecting data (e.g., wave loads or hull vibration) for research within a field. Different classification societies use different notations and groupings for hull monitoring. Two examples of the different applications for a hull-monitoring system can be found in H-MON by DNV and "Guide to hull condition monitoring" by ABS, with common applications, such as strain measuring on hull girders, accelerometers in the bow and aft in order to assess risks for slamming, and propeller emergence, DNV (2011) and ABS (2003).

4.2 Ice load monitoring

One identified challenge has been the lack of information to the bridge about the actual load on the hull. As ice load exceeding the design load of the ice class is a major risk for any ship travelling in ice-infested waters, which is an effect of the unpredictable nature of ice loads, and these loads may cause permanent damage to the ship structure and interrupt operations, Mejlaender-Larsen and Nyseth (2007).

One hull-monitoring system specified for ice loads, ABS (2011) offers the additional notation ILM for ice load monitoring. It is used for providing the bridge with near real-time information on the measured data when transiting in ice, warning the vessel's personnel if measured parameters approach the permissible levels and warning the vessel's personnel if the conditions imply a trend towards permissible levels, based on a recent impact. The ILM is based on information provided by strain gauges, which are applied to the ship's structure based on what is to be measured. The basic ILM system includes only hull stress monitoring but can be extended to include turning loads in ice, global ice loads, local ice forces and local ice pressures. Similar to the ABS ILM notation, DNV also has the extension ILM to the H-Mon notation. The DNV system contains:

- Strain sensors to measure the strain at the frames (i.e. the actual structural response).
- Electro-magnetic ice thickness measurement equipment.
- Software to process the measured information.
- Possibility to apply metrological and satellite data and apply these on electronic sea charts.
- Display and update the ice information forecast continuously.

For an illustration of how the equipment is used on a vessel, see Figure 4.1. When measuring the global ice-induced forces according to ILM, strain gauges are placed to measure the strain in the deck and major hull girder plates. This is the conventional method for deciding ice loads on the global structure. The strain sensors are accurate and well proved as a measuring method, but, on the negative side, it is a tedious job to install such equipment on a vessel, Johnston et al. (2003).

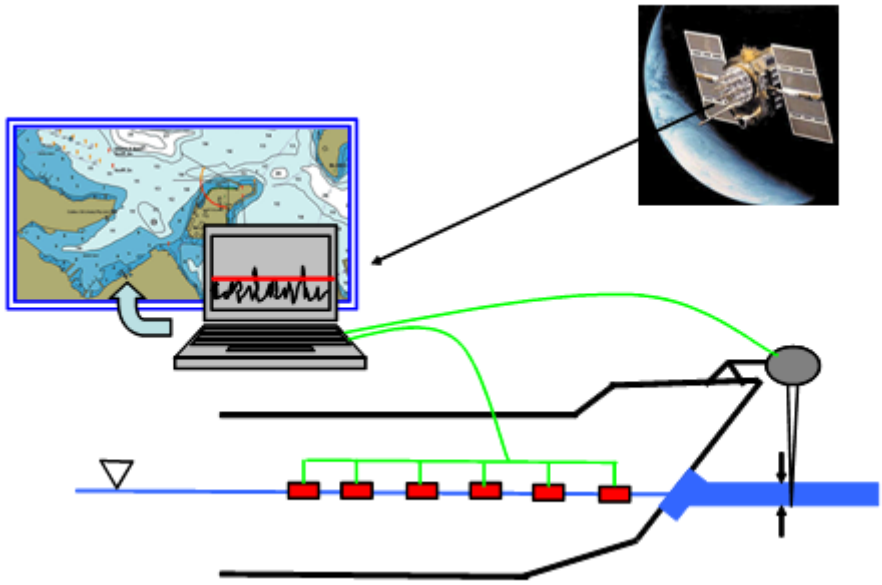

Figure 4.1 *DNV ILM equipment. The ellipse indicates the location of an electro-magnetic ice thickness measurement unit; squares illustrate strain sensors mounted on the hull. Information from the equipment is processed in a computer on the bridge.*

Another method for calculating global ice- induced forces has been the subject for research work, mainly at the Canadian Hydraulic Centre within the National Research Council of Canada in the late 1990s and early 2000s. This method uses the ship's global accelerations and the equation of motions to compute the global force that must have been the source of the sudden change in speed and direction of the ship, with the assumption that the body behaves like a rigid body, Johnston et al. (2001).

One major advantage with motion analysis compared to more traditional ILM with strain sensors, is that the installation of instruments is easier and needs less time, compared to mounting one unit somewhere in the ship to install 66 strain sensors,

Mejlaender-Larsen and Nyseth (2007). On the other hand, the possibilities of estimating the local strains are eliminated, and as the ship does not behave entirely like a rigid body, the bending and twisting of the ship's hull can result in inaccurate measurements.

In 2000, the Canadian Hydraulic Centre started measuring the motions of USCGC Healy during ramming of heavy ice features. Using the linear equation of motions it was possible to calculate the global forces induced on the ship's hull by the ice. The motion- measuring unit is called MOTAN (short for motion analysis) and consists of the measuring unit and a software package for computing the forces. The measuring units include three accelerometers that measure the translational accelerations (m/s^2) in the Cartesian coordinate system and three angular rate sensors that measure the angular velocity (rad/s) about each Cartesian axis. To date, MOTAN has been used on several icebreakers from both the US and Canadian Coast Guards, Santos-Pedro and Timco (2001), Johnston et al. (2003) and Johnston et al. (2004).

The motions are filtered using a 5 Hz low pass filter in order to eliminate additions springing from non-rigid body motions, i.e. vibrations. The velocity and displacement in the translations are computed by numerical integration of the accelerometer results, and similarly the measurements from angular velocity are transformed to acceleration and displacement by derivation and integration, respectively. The low pass filter frequency of 5 Hz is chosen since the rigid-body ship motions are typically in the low frequency range, below 3 Hz, Chen et al. (1990). MOTAN was originally placed on ship models during testing in towing tanks, Miles (1986), and proved to be accurate in the trials. When put on USCGC Healy in the year 2000, the measured motions could be verified from other motion- measuring tools, Johnston et al. (2001). Since then the system has been put to use on several other icebreaking ships and the results are concluded in Appendix B.

The work of estimating the forces from an inertial measurement system is motivated by the simplicity of installing such a device on any ship. Hence the data-gathering procedure is easier than the previous work that has been done by way of installing strain sensors along the ice belt.

A less documented study has been made on the Russian icebreaker Kapitan Nikolaev, Likhomanov et al. (2009) and Krupina et al. (2009), similar to the study on Terry Fox, Johnston et al. (2003), where both strain measurements and inertial measurements methods where used. The forces were computed by taking the rudder angle and propulsion into account when computing the forces in the surge and sway direction. The results of the study are, however, sparsely presented due to a request from the customer to keep the result a commercial secret. The conclusions of the study are that the major force contribution is from the vertical component followed by the component in the surge-direction; the sideways component seems to be of negligible magnitude.

4.3 Ice-load monitoring on KV Svalbard

KV Svalbard is owned by The Norwegian Coastguard, and it is assigned as a DNV ice class POLAR-10 Icebreaker and is designed to operate in first-year and multi-year ice with thicknesses between one and two metres. The stations are the Arctic waters north of the Norwegian mainland, the Barents Sea and the areas around the Svalbard

islands, DNV (2009). Main particulars of KV Svalbard can be seen in Table 4.1 below.

Table 4.1 Main particulars KV Svalbard.

Main particulars	Value
Length over all	103.7 [m]
Length between perpendiculars	89.0 [m]
Breadth	19.1 [m]
Draught	6.5 [m]
Displacement	6500 [ton]

KV Svalbard was the first vessel to be equipped with DNV's ice-load monitoring system, and the first sea trials were completed in the winter of 2006-2007, Mejlaender-Larsen and Nyseth (2007). The equipment was as described in Chapter 4.2. As an extension of the ice-load monitoring programme, KV Svalbard was equipped with a Motion Response Unit (MRU), Kongsberg (2006). The MRU is similar to the MOTAN unit used by Johnston et al. (2001). The MRU is developed and manufactured by Kongsberg AS. The model installed on KV Svalbard is the Seatex MRU-H. The MRU is capable of recording all motions (acceleration, velocity and displacement) in all six degrees of freedom (surge, sway, heave, roll, pitch and yaw) to give the complete picture of the ship's rigid body state. The MRU is located at the bridge 20.4 m forward, 15.1 m above and 1 m starboard of the ships' centre of gravity.

When the MRU is active and records the motion data, the records are based on accelerations in translational motions, i.e. the accelerations in surge, sway and heave, and the velocity and displacement are deduced by numerical integration. In the rotational motions, the velocity is measured and the accelerations are found by the numerical derivative, displacement by numerical integration, Kongsberg (2006). The MRU configuration used in the trials records motion in 16 channels. This means that during the trials, two motions were to be excluded from the records. The motions that were excluded are velocity and displacement about the x-axis (roll). This can be motivated by an assumed negligible effect on the global forces on the rigid body motions provided by a square impact, Johnston et al. (2006).

The MRU used works with a sampling frequency of 100 Hz and a recording frequency of 25 Hz. According to the Nyqvist sampling theorem, a signal can be sampled only if it does not contain frequency components above one-half of the sampling rate. For the MRU output this would mean that only frequencies below 12.5 Hz can be contained properly within the data to prevent aliasing, Smith (2003). According to Chen et al. (1990), the rigid body motions have natural frequencies lower than 3 Hz and hence can be properly contained in the 25 Hz sampling frequency. The MRU model used is designed to measure motions of marine structures with high accuracy in the vertical direction. In horizontal directions it is only suitable to measure rather fast motions.

To measure acceleration and after that integrate twice for obtaining translation puts high requirements on the accuracy of measured acceleration. The main problem is to remove the gravity acceleration component from the measured acceleration. It is much easier to remove the gravity component in the vertical than in the horizontal direction, since a small error in roll or pitch angle gives a larger error in horizontal than vertical acceleration. The error is of the first order in the horizontal and of the second order in the vertical direction.

In order to assess the effects of errors contained and amplified in the integration process, a Kalman filter is used in the internal processing of the integration. The Kalman filter is applicable on a linear dynamic system like this, and assuming that the error terms have a Gaussian distribution, gives an estimate of the system's actual state. This means that the better the noise estimation is known, the more reliable the data output will be, Welch and Bishop (2006). For the measured accelerations, however, the filter process is left out; leaving an output that is in need of post-treating.

When assessing the rotational motions, the Kalman filter is only applied on the integration from velocity to displacement. The MRU rotational velocities consist of the same type of high-frequency noise as the translational accelerations described above. When the velocity is derived to accelerations, the amplitude of the high-frequency noise will increase and the impact of the noise will be amplified by the derivative operation. Mathematically this can be explained by considering the simple sine wave $f(t) = A\sin(\omega t)$. The amplitude of its derivative will be $A\omega$ as $f'(t) = A\omega\cos(\omega t)$. Hence, a noise with a high frequency will affect the derived acceleration to a greater extent than a low-frequency noise. For this reason, it is important to remove the noise in the velocity before deriving the accelerations. This is not done internally in the MRU.

Examples of typical measurement records are shown in Figure 4.2, where the motions in the heave and pitch direction are plotted over a two-second long interval. As can be seen, the Kalman filter removes the high-frequency parts in the integration process (displacement and velocity in heave, and displacement in pitch), but for the measured values (acceleration in heave and velocity in pitch) and the derivative (acceleration in pitch) the high-frequency noise remains.

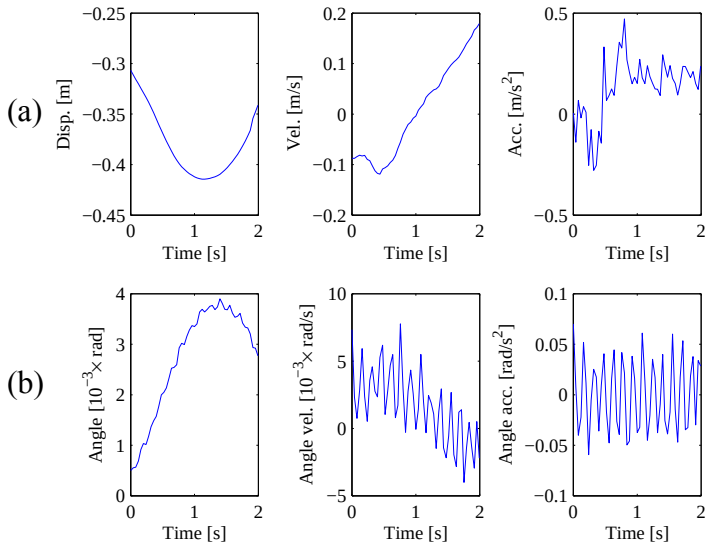

Figure 4.2 *Typical measurements of a) translational (heave) and b) rotational (pitch) motions by MRU in (from left) displacement, velocity and acceleration.*

5 Computational model

This chapter describes the model used for post-processing data from MRU measurements and computing the forces. It was done according to the method described in Figure 1.3, Chapter 1.3. First, the process of removing the noise and the influence of the filtering process is described, followed by the process of transferring the motions from the MRU position to the centre of gravity. Finally, the process of computing the forces and identifying the ramming events is presented.

5.1 Post treatment of measurements

The methodology used in the current work is based on the assumption that the ship behaves like a rigid body. In reality, however, the ship is not a rigid body, and the motions can be divided into the rigid-body motions and the elastic-body motions. When encountering external loads, the corresponding motions will be the rigid-body motions (surge, sway, heave, roll, pitch and yaw), elastic-body motions and quasi-static bending of the hull girder. The elastic-body motions will be of an oscillating character, i.e., vibrations. The quasi-static bending of the hull girder will be neglected, since the ship is considered to be in equilibrium before impact and only the first impact is considered. Vibration is defined as a relatively small amplitude oscillation about a rest position, Lewis (1988). These oscillations will be measured by the MRU and will hence introduce a measurement error. The rigid- body motions of heave, pitch and roll are also oscillations around a rest position but are not referred to as vibrations. As explained in Chapter 1.4 only the rigid-body motions should be included in the force computation.

In order to separate the rigid-body oscillations from the vibrations one can look into the ship's natural frequencies. A natural frequency is a frequency at which a system vibrates when stimulated impulsively from the rest position. The requirement for natural vibration is that the system possesses both mass and stiffness. For a continuous mass and stiffness system an infinite number of natural frequencies exist, however, only a few of them are of practical interest, Lewis (1988).

In Fredriksen (2012), the natural frequencies of KV Svalbard have been estimated for the different bending modes, see Table 5.1. The natural frequencies are computed with a simplified beam FE-model. The results can be compared to Chen et al. (1990), where they state that motions above 3 Hz typically originate from vibrations. From the results below it seems that the rigid-body motions are even lower in range; with pitch at a natural frequency of 0.17 Hz; and heave at 0.16 Hz; and the first vibrational mode with a natural frequency of 0.83 Hz.

Even though the natural frequencies are computed by a simplified model, the conclusion that vibrations have a higher frequency than the desired rigid-body motions can be reached. Therefore, a low pass filter is appropriate for removing the vibrations from the data.

Table 5.1 Natural frequencies of KV Svalbard, Fredriksen (2012).

Mode	Natural frequency [*Hz*]	Natural Period [*s*]	Comment
1	0.16	6.07	Rigid body heave
2	0.17	5.99	Rigid body pitch
3	0.83	1.21	2-node bending
4	2.22	0.45	3-node bending
5	4.16	0.24	4-node bending
6	6.67	0.15	5-node bending

As the method to compute the natural frequencies is a simplification of the real case, a study of using different cut-off frequencies in the low-pass filtering is performed in order to investigate the feasibility of the results presented in Table 5.1. The results from the different cut-off frequencies are presented in Figure 5.1 where the pitch acceleration amplitude is shown on the y-axis, over a 10- second long interval, where the vertical line indicates one of the given impacts (for the impacts, see Chapter 5.3).

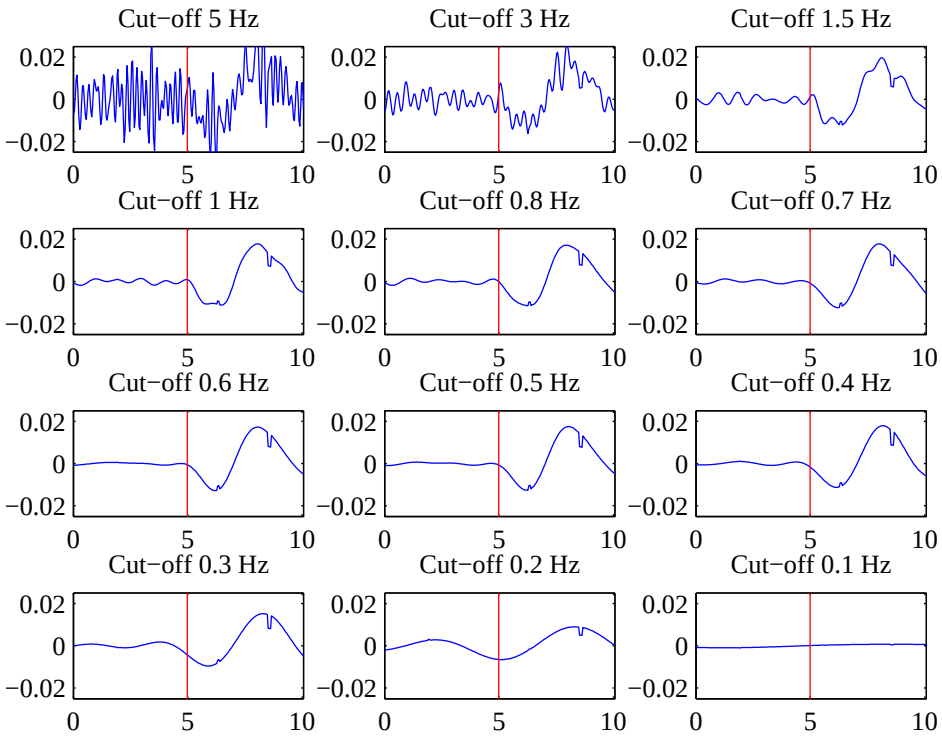

Figure 5.1 Comparison between different low-pass cut-off frequencies with pitch acceleration on the y-axis, time on the x-axis and impact indicated by the vertical line.

From Figure 5.1 it can be concluded that the 5 Hz low-pass filter used by Johnston et al. (2001) in the MOTAN project will still consist of a high volume of noise if applied on the MRU data. This can be explained by both a 3-node and 4-node bending for KV Svalbard being below 5 Hz, as observed in Table 5.1. It is when the cut-off frequency approaches 0.8 Hz that the smooth curve that characterizes the slow motions of a ship's movement occurs. If the cut-off frequency is too low, the amplitude response gets smaller, and, at a 0.1 Hz cut-off frequency, almost all motions are removed. This is because the filter starts to remove the low-frequency parts, which are the pitching motions, and hence is a too low filter cut-off frequency. From this reasoning, a low-pass filter cut-off of 0.6 Hz is chosen, as it lies well below the 0.83 Hz 2-node bending natural frequency, and does not interact with the amplitude response of the pitching motions.

5.2 Computation of forces

From the MRU-configuration file it can be read that the unit is installed in a distance (x, y, z) from the centre of gravity. This means that in order to apply the force computations described in Chapter 1.3, we need to translate the measured motions into the corresponding motions in the centre of gravity, see Figure 5.2 for the MRU position and the location of centre of gravity.

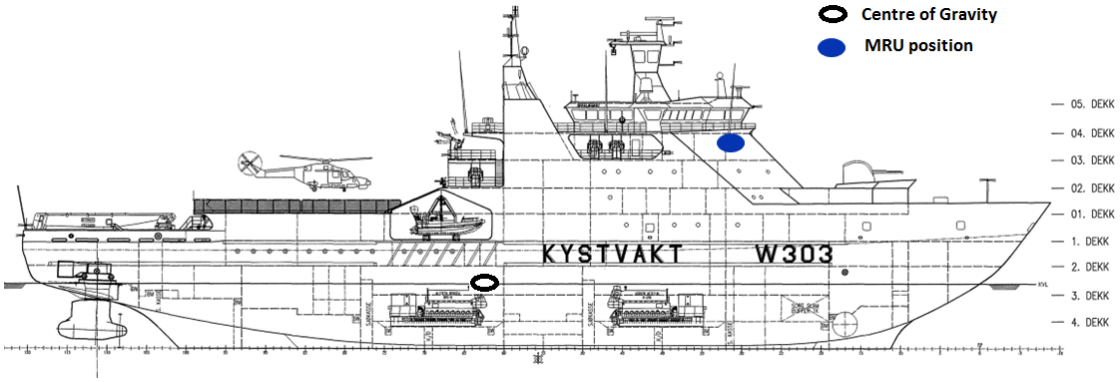

Figure 5.2 Location of MRU position (solid ellipse) and distance to centre of gravity (empty ellipse).

This is done by using the relation of motions of a fixed point on a rigid body as in equation 5.1. Equation 5.1 is a linearized equation valid for small angles (less than 10°) for pitch, heave and yaw, Jansson (2011). As presented in Chapter 6, the measured angles lie within this assumption.

$$\begin{bmatrix} \eta_{1,COG} \\ \eta_{2,COG} \\ \eta_{3,COG} \end{bmatrix} = \begin{bmatrix} \eta_{1,MRU} + z\eta_{5,MRU} - y\eta_{6,MRU} \\ \eta_{2,MRU} - z\eta_{4,MRU} + x\eta_{6,MRU} \\ \eta_{3,MRU} + y\eta_{4,MRU} - x\eta_{5,MRU} \end{bmatrix} \tag{5.1}$$

When looking upon the forces acting on a ship, there are external forces ($\mathbf{F}_E$) such as thrust, wave forces, ice loads etc. that act with an accelerating effect on the ship. We also have the hydrodynamic reaction forces ($\mathbf{F}_R$) that are the effect from resistance and elevated displacement (in heave, pitch and roll).The sum of forces can be put into

Newton's second law, equation 5.2. Observe the added mass, $\mathbf{A}$, which is an effect of the acceleration of the water around the ship, Jansson (2011).

$$\mathbf{F} = \mathbf{F}_R + \mathbf{F}_E = (\mathbf{M} + \mathbf{A})\ddot{\eta} \tag{5.2}$$

In mechanical representation this can in the one-dimension case be looked upon as a linear mass-spring-dampened system, which, together with the corresponding free-body diagram is shown in Figure 5.3.

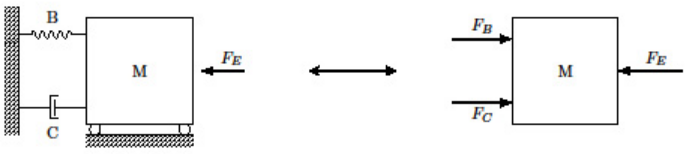

Figure 5.3 *Free-body diagram of a 1D dampened spring mass system which is used to illustrate the forces acting on a ship body moving in water in heave, pitch and roll directions.*

In Figure 5.3 above, the hydrodynamic reaction force is divided into the damping forces $\mathbf{F}_B$ which are dependent on the ship's velocity and the hydrodynamic stiffness $\mathbf{F}_C$ which is dependent on the ship's displacement. Thus Equation 5.2 can be developed to equation 5.3, Jansson (2011):

$$\mathbf{F} = \mathbf{F}_E - \mathbf{F}_B - \mathbf{F}_C = (\mathbf{M} + \mathbf{A})\ddot{\eta} \leftrightarrow (\mathbf{M} + \mathbf{A})\ddot{\eta} + \mathbf{F}_B + \mathbf{F}_C = \mathbf{F}_E \tag{5.3}$$

If the components of $\mathbf{F}_E$ are investigated, it can be assumed that the forces that are acting on the body are wave forces, thrust from the propeller and ice loads. However, as a limitation of this thesis, it is assumed that there is no varying wave force acting on the ship, the thrust and ship resistance are assumed to be constant and the influence of the rudder is neglected. From this, only the ice forces remain in Equation 5.3 and can be used for computing the external ice loads. With linearized equations for $\mathbf{F}_B$ and $\mathbf{F}_C$ and the matrix formulation for the linearized equations of motions for exciting force $\mathbf{F}_E$, becomes clear from Equation 5.4, Jansson (2011).

$$\mathbf{F}_E = (\mathbf{A} + \mathbf{M})\ddot{\eta} + \mathbf{B}\dot{\eta} + \mathbf{C}\eta \tag{5.4}$$

Further analysis of the different components in the force vector $\mathbf{F}_E$ gives, $F_1 - F_3$ representing the forces acting on the ship's COG, and $F_4 - F_6$ representing the moment about each axis at the ships COG. It is possible to translate these forces into the forces that are acting on the bow by dividing the moment by the corresponding lever. Hence, it is possible to describe either the force acting on the ship's centre of gravity (COG) or the corresponding force acting on the bow (POI). The force resultant is computed in the same way for both POI and COG, see Equation 5.5 below:

$$F = \sqrt{F_1^2 + F_2^2 + F_3^2} \tag{5.5}$$

But the difference for COG is that the forces are inserted from Equation 5.4, while for POI the forces from Equation 5.6 are used. x_{COG}, y_{COG} and z_{COG} are the distances from the point of impact to the ship's centre of gravity.

$$\begin{aligned} F_1 &= F_1 \\ F_2 &= F_5 / z_{COG} + F_6 / x_{COG} \\ F_3 &= F_4 / y_{COG} + F_5 / x_{COG} \end{aligned} \tag{5.6}$$

Since z_{COG} is assumed as being small (i.e. centre of gravity close to water plane and thereby also impact) and since the motions around the y-axis are small (small roll motions due to a square hit), the resulting forces F_{COG} and F_{POI} can be written as in equation 5.7, by combining Equation 5.5 and Equation 5.6.

$$\begin{aligned} F_{COG} &= \sqrt{F_1^2 + F_2^2 + F_3^2} \\ F_{POI} &= \sqrt{F_1^2 + \left(F_6 / x_{COG}\right)^2 + \left(F_5 / x_{COG}\right)^2} \end{aligned} \tag{5.7}$$

5.3 Event identification

The data collected from the MRU contains several hours of motion recordings. An important step is to choose which time intervals are of interest for this study. Given the notes from one day of trials, Nyseth (2012), several ice collisions are clocked in, some with notes of the ice conditions, i.e. ice ridge, large floe, ice edge, etc. However, some of the collisions are noted to be ramming of heavier ice features, such as ridges, when the vessel is already in an icebreaking operation and some of the collisions have large motions before a noted impact.

As has been stated in the limitation of this thesis, it is assumed that the ship hits an ice feature from open water. An assumption in Equation 5.4 is that all forces from other external sources than ice are zero. Taken together, this means that the motions before the impact should be small. This means that when there are large motions before the supposed impact, it cannot be excluded that the ship is either breaking ice or is affected by some other external force. If the ship is already in an icebreaking operation, the assumption that the ice force acts in the bow is not valid.

In either case, motions before the supposed impacts means that the model is not valid for use and this has implied that several indicated collisions that were noted during the trials were discarded, as our assumptions were obviously not valid. This assessment was done manually for each one of the hits. Figure 5.4 shows the motions of Event 1 and Event 4 from Table 5.2. Event 1 is an example of when the ramming incident is considered to fulfil the model and Event 4 is an example of motions before the impact, which makes the incident inapplicable for the model. The impacts in Table 5.2 were chosen to evaluate the model.

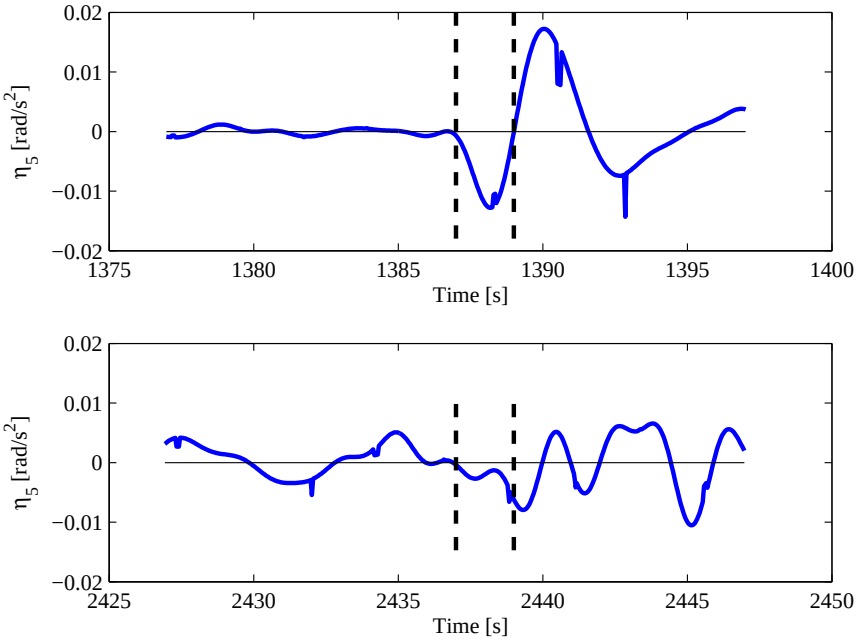

Figure 5.4 Solid lines indicating pitch accelerations for Event 1(upper) and Event 4 (lower). Left dashed line indicating impact and right dashed line the stop of the considered interval. Observe the large accelerations before impact for Event 4.

Table 5.2 Impacts for evaluation.

Event number	Date and Time (YYYYMMDD_HHMMSS)	Comment
1	20120316_092307	Open water to ridge
2	20120316_124721	Large block
3	20120316_125424	Open water to ice edge
4	20120316_134037	Open water to ice edge

Event 1 and Event 3 are chosen as they are impacts with small motions before impact and the collision results in small translations in sway and small rotations in roll and pitch. It seems as if they fulfil the limitation of the model and measuring unit that it is only valid for squared hits.

Event 2 is chosen because it also has small motions before the impact and the collision results in a clear response in the measured data. However, this event is a collision with a large ice block and it gives large responses in sway and yaw. This indicates that the hit is not square. This event is therefore only used to compare with Event 1 and Event 3.

Event 4 should, according to the comments, Nyseth (2012), be a good hit when the ship comes from open water and collides with an ice edge, but there are large motion responses before the impact and therefore it cannot be excluded that the ship is under influences of other forces than ice loads. Therefore, this event is acknowledged as an example of when the model is not valid.

6 Results and discussion

The following chapter presents, analyses and evaluates the results of the model. The impacts that were chosen for processing in the model were chosen as explained in Chapter 5.3. The motion responses are presented and discussed, followed by a discussion of the computed forces.

6.1 Motion response amplitudes

Since the motion response is the source of the computations an evaluation of all motions in the 6 DOF has been carried out. The motion response on impact can be found in Table A.1-3 in Appendix A, and for Event 1 in Table 6.1 below. It can be seen that for Event 1, the major motions are surge, heave and pitch while sway, roll and yaw are small. This is a good result since it confirms that Event 1 is a squared impact. However, the displacement in yaw and sway are large compared to all other displacements. This can be explained by difficulties with measuring the two, as they are relative to the ship-based coordinate system. As explained in Chapter 4.3, the MRU needs input of heading and position in order to create accurate predictions of yaw and sway displacement and that input was not used during the trials. This has, however, no impact on the force results, as displacement in yaw and sway are not a cause of any counteracting forces or moments, as the case is, for example, for heave and pitch.

Table 6.1 Maximum motion response on impact for Event 1.

	Surge	Sway	Heave	Roll	Pitch	Yaw
Disp.	0.38 [m]	10.56 [m]	0.20 [m]	-	-0.170 [°]	-29.501 [°]
Vel.	-0.19 [m/s]	-0.09 [m/s]	0.21 [m/s]	-	-0.688 [°/s]	0.115 [°/s]
Acc.	-0.30 [m/s^2]	-0.10 [m/s^2]	0.32 [m/s^2]	0.057 [°/s^2]	-0.630 [°/s^2]	0.115 [°/s^2]

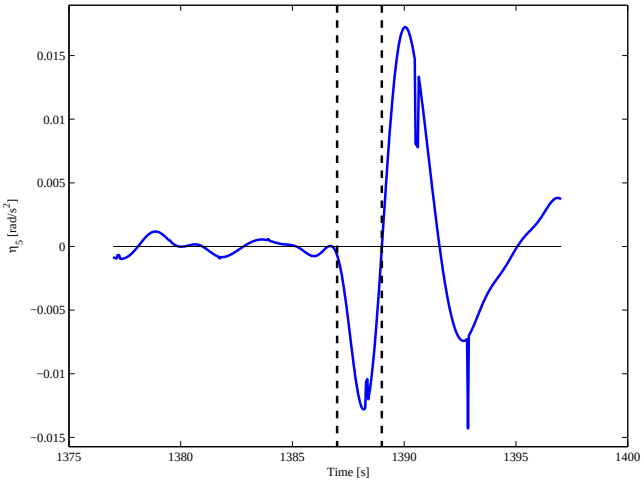

Figure 6.1 Pitch acceleration (solid line) before (to the left of the dashed lines), during (between the dashed lines) and after (to the right of the dashed lines) Event 1.

An example of the pitch acceleration response before, during and after Event 1 is displayed in Figure 6.1. The solid curve shows the pitch acceleration and the dashed line marks the impact interval. It can be seen that there are small accelerations before the impact. On impact there is a clear response with a negative pitch acceleration, which, in the chosen coordinate system, means that the bow accelerates upwards. After the impact interval the bow accelerates downwards, which indicates that the ice has failed and the ship moves back downwards.

This can be compared with the corresponding response for Event 4 in Figure 6.2. There is a negative response in pitch in the impact interval, but it is small compared with the response in Event 1. More importantly, it cannot be excluded that there are forces acting on the hull before the noted impact time, as there are several motions before the impact interval.

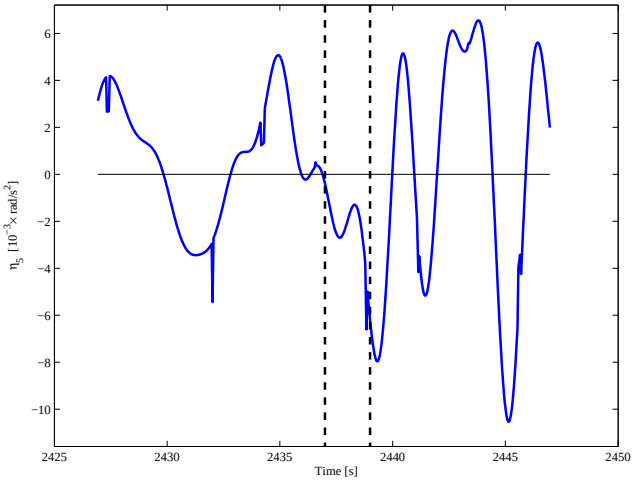

Figure 6.2 Pitch acceleration (solid line) before (to the left of the dashed lines), during (between the dashed lines) and after (to the right of the dashed lines) Event 4.

As previously discussed, the MRU used allows for the external input of speed, position and heading information, and this is to both give more information to the user, but also to improve accuracy of the motions, Kongsberg (2006). During the trials at KV Svalbard this function has not been used, which reduces the accuracy of primary surge, sway and yaw, Kongsberg (2006).

6.2 Computed forces

The forces are calculated as described in Chapter 5.2 and can be divided into one part from the accelerations, one part from the velocity and one part from the displacement. All numbers of how much each part contributes to the total force can be seen in Appendix A. The maximum forces and moment due to displacement, velocity and acceleration for Event 1 are presented in Table 6.2. The forces and moments due to displacement in the surface plane are all zero, as the motions do not cause any restoring forces to arise. The forces and moments caused by velocity are also small, and the dominating contribution is the acceleration sources. This is expected as the ship is considered to be at an equilibrium when it hits the ice edge. This means that the values of the displacement and velocities will be low during the whole interval.

Table 6.2 Maximum force and moments during Event 1.

F_{part}	F_{surge} [MN]	F_{sway} [MN]	F_{heave} [MN]	F_{roll} [MNm]	F_{pitch} [MNm]	F_{yaw} [MNm]
Disp.	0	0	2.75	-	-11.52	0
Vel	-0.12	-0.06	-1.59	-	-15.15	-1.43
Acc	-2.65	-1.05	8.34	0.62	-175.5	19.64

To further analyse how the forces are put together, the forces are split up into the 3 principal direction components, as seen in Table 6.3 and Table 6.4. Table 6.3 shows the contributors to and the force resultant at the centre of gravity and Table 6.4 shows the contributors to and the force resultant at the point of impact. It can be seen that the governing contribution to the force resultant for Event 1 is the contribution in the z-direction, the second is the x-direction and the least contribution to the force resultant gives the force in the y-direction. This is an expected result since this is a head-on impact, which gives low reactions in the y-directions. This is also the same result as Krupina et al. (2009) and Johnston et al. (2001) achieved when they carried out similar tests.

Looking into Event 2, it can be seen that the forces in the y-direction are proportionally greater. This can be explained by a non-square hit. This makes the calculated forces more unreliable since the measurement unit has less accuracy in this direction and the lever to the centre of gravity is uncertain. Event 3 also has quite a great influence from the force component in the y-direction, which indicates that the hit is not completely squared. However, the components in the x- and z-directions are still in the same order. The same holds for Event 4.

Table 6.3 Maximum force components and resultant in the centre of gravity during the impact interval.

Event	Fx_{COG} [MN]	Fy_{COG} [MN]	Fz_{COG} [MN]	F_{COG} [MN]
1	-2.67	-0.99	8.46	8.81
2	-1.79	8.45	2.52	10.63
3	-1.45	2.88	4.34	6.19
4	-1.06	1.37	1.65	2.62

Table 6.4 Maximum force components and resultant at the point of impact during the impact interval.

Event	Fx_{POI} [MN]	Fy_{POI} [MN]	Fz_{POI} [MN]	F_{POI} [MN]
1	-2.67	0.37	4.77	5.34
2	-1.79	-3.03	4.38	6.51
3	-1.45	-1.56	1.85	3.04
4	-1.06	-0.30	0.70	1.68

One remarkable thing is the difference in magnitude between the force resultant at the centre of gravity compared with the point of impact. The force resultant at the centre

of gravity is between 49% and 64% larger than the resultant at the point of impact. According to the rigid body assumption, these force resultants should be equal. As explained in Chapter 5.2, the force components in the longitudinal direction are the same at both the centre of gravity and at the point of impact, so the error originates from the forces in the y- and z-directions. The difference between the corresponding two has approximately the same ratio as the difference between the resultants.

One of the sources of this difference could be the difference in measurement performance, as the forces at the centre of gravity are calculated from the translational accelerations, but in the case of the point of impact, the forces are based upon the rotational accelerations in the yaw and pitch direction. This problem was also found by Johnston et al. (2001) and their conclusion was that the measurement accuracy was superior in the rotational measurements and therefore the point of impact was more accurate. They also verified their measured motions by complementing inertial measurements.

In this case, it is stated in the MRU manual, Kongsberg (2006), that the MRU model used in the trials on KV Svalbard is "specially designed for motion measurements in marine applications requiring highly accurate heave measurements". The resolution of the measurement accuracy noted for the motions is high when compared with the maximum motions in these events. Kongsberg Seatex, which manufactures the MRU, states that the MRU needs to be calibrated every five years to maintain specified accuracy. According to the MRU configuration files, the last calibration of the MRU on board KV Svalbard was done in 1999. The accuracy of the measurements done in 2012 is therefore uncertain.

This gives a large uncertainty to the numbers in the result and it cannot be certain which result is the more correct. As the heave is supposed to be accurate it can be speculated that the COG results are better. However, as none of the MRU-measurements can be confirmed by any complementing measurements, the accuracy of the results cannot be assessed thoroughly. It is still of interest in attempting to decide how good the model is if we disregard the problems with confirming the accuracy of the measurements. The magnitude of the forces can still be compared with the ice class rules and other similar studies in order to confirm that the results end up in a feasible area. To compare the force resultants, the design force in ice class rules are calculated. It is calculated with the following assumptions according to DNV (2012):

- All geometrical variables estimated from drawings.
- Vertical distance from COG to upper ice water line equals zero.
- Collision is at the forward perpendicular.

The results are compared with each maximum point of impact force during the impact interval in Table 6.5 below. As can be seen, the design forces calculated by the ice class rules are much larger than the calculated force resultants both at the centre of gravity and at the point of impact. The design forces are based upon a glancing impact, which is a single impact; this is same as the force calculated in the impact interval by the model. As the conditions during impact are unknown it cannot be known if the calculated force lies close to or far away from the design load. If the

forces calculated are the forces experienced, every normal impact of the design load is probably too low, but if the calculated force is during an extreme collision event there is a better safety margin.

Table 6.5 Maximum force resultant in POI and COG during the impact interval compared with the design force by DNV (2012).

Event	F_{POI} [MN]	F_{COG} [MN]	F_{POI} DNV [MN]
1	5.336	8.809	18.118
2	6.511	10.633	18.118
3	3.044	6.193	18.118
4	1.678	2.618	18.118

The calculated forces can also be compared with previous MOTAN studies performed by Johnston et al. (2001) and Johnston et al. (2003). A short summary of those results can be found in Appendix B. The results from the MOTAN project are in the same order of magnitude as the result from the model presented above in this thesis. The values during the MOTAN trials are a little higher in numbers. This is expected as the ships in the MOTAN trials have about twice the displacement and included hits with smaller icebergs, which causes higher forces than an ice edge as the small iceberg tend not to break in a collision. As the impacts type and impact speeds are unknown for Events 1 to 4, it is hard to draw any further conclusions from this comparison other than that the forces calculated are in the same order and therefore seem reasonable.

As stated in Chapter 2, the force plot should have a saw-tooth shape, this because of the crushing and bending failure of the ice. As can be seen in Figure 6.3 the force alternates; the force increases until the ice breaks and subsequently the force increases again until the next failure. However, the frequency is quite low, which means that the force mainly consists of the force from the bending failure of the ice rather than the crushing failure. The crushing part can be seen as a more or less constant force when it is integrated over the impact area on the hull.

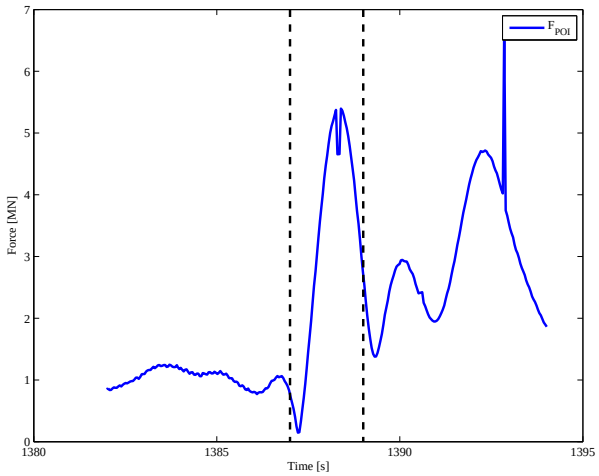

Figure 6.3 Force resultant at the point of impact for Event 1.

In addition to the comparison with previous results and the design load, an external mechanical analysis of the collision was performed. A complete external mechanic model would need good measurements of the relative velocity between the ship and the ice feature. In the case when the ship collides with an ice edge, the relative velocity is the velocity of the ship towards the ice edge, which simplifies the measurements. Unfortunately, the data given does not have any accurate measurements of the ship's velocity even if the collision is assumed to be squared. The dissipated energy in the collision cannot be calculated, but the theory behind external mechanics can be used for estimating the velocity that would have been lost in our collisions. This velocity can be used as an aid to see if the forces are of reasonable size.

A simplified external mechanical analysis of the collisions has been made where the force calculated above is used for calculating the momentum before and after the impact. The difference in momentum is then used for calculating the velocity difference that the computed forces would result in. During the calculations the following assumptions have been made:

- No dissipated energy, which means an elastic collision.
- Collision with an ice-edge, which means no ice velocity.

The velocity change in the bow can be seen in Table 6.6 and it can be seen that the velocity changes seem reasonable as the total velocity change are largest upwards and forward, which are in accordance with the reasoning in Chapter 2.3.

Table 6.6 Velocity change in the bow for the different impacts based on simplified external mechanical calculations.

Event	x-direction [m/s]	y-direction [m/s]	z-direction [m/s]
1	-0.67	0.30	1.75
2	-0.32	-1.13	0.64
3	-0.25	-0.45	0.26
4	-	-	-

If the velocity measurements had been better, a deeper external mechanical analysis would have been possible. Then the dissipated energy could have been calculated and the forces could have been verified.

7 Conclusions

Measurements of a ship's motions can be used for increasing the knowledge of the factors that affect a ship travelling in ice-infested waters. The motions can be used for calculating the global forces that affect the hull when colliding with ice features. These measurements give information that makes it possible to create safer ship designs and to manoeuvre the ship more safely in ice- infested waters.

The objective of the thesis was to create a model that from measured rigid-body ship motions computes the global forces acting on the ship's hull when colliding with heavy ice features. The model created performs these computations. It calculates the ice-induced global force on the ship's hull both at the centre of gravity and at the point of impact.

The created model is based on well-established equations. It has been compared with both design loads from ice class rules and with results from previous studies. From this comparison it can be concluded that the model seems to give reasonable values of the calculated force. However, it has not been possible to verify the model. This is because the measured motions used as inputs have not been verified and other measurements that could be used for verifying the magnitude of the calculated force are missing.

Using the global responses, as was done in this model, one must be aware of the limitations and prerequisites of the ship's state pre impact in order for the model to be applicable. The limitations for this model make it suitable to analyse ice impacts that are similar to the impacts used as design load for the IACS unified polar class rules. A further development of the model would also make it possible to use it to give real-time feedback to the bridge about what ice forces are acting on the hull.

The forces acting on a ship's hull when ramming a heavy ice feature are mostly governed by the acceleration of the ship body. The largest force component for a square impact is the force in the vertical direction followed by the force in the longitudinal direction. The force in the transverse direction is the smallest. If the impact is oblique, the force component in the transverse direction contributes more.

8 Future work

The objective was to create a computation model that calculates the global ice-induced force from the rigid body motions of the ship. This model has been made, but there is lack of verification of the results. In order to verify the results, additional trials are needed.

One of the main concerns regarding verification of the results is that there is no verification of the MRU measurements. It is necessary to keep independent measurement devices to compare with the MRU measurements, as well as keeping the MRU well calibrated during each trial. Several MRU units could be placed around the ship, where the primary MRU is close to the centre of gravity. This is another way of providing the possibility to judge the accuracy of the MRU. The MRU has the possibility to input position and heading information from GPS. This should be used in order to ensure better accuracy in yaw, surge and sway measurements. If more accurate velocity measurements were made a more thorough external mechanic analysis of the collisions could be made. This analysis could subsequently be used to simulate ice collisions.

KV Svalbard is equipped with an ILM system. The strain sensors of the ILM system should be active to provide additional methods to estimate the global forces. Additionally, impact pads could be used for providing more information about the impact location and estimates of the global force.

Conditions during each of the hits should be described in more detail in order to provide an understanding of the difference in load case depending on the ice-impact scenario. All this could be used in order to develop and verify the model.

9 References

ABS (2003): *Guide for hull condition monitoring systems*, American Bureau of Shipping, Houston, Texas, 2003, 19 pp.

ABS (2011): *Guide for ice load monitoring system*, American Bureau of Shipping, Houston, Texas, 2011, 14 pp.

Bintanja, R., van Oldenborgh, G. J., Drijfhout, S. S., Wouters, B., Katsman, C. A. (2013): Important role for ocean warming and increased ice-shelf melt in Antarctic sea-ice expansion, *Nature Geoscience,* March, 2013

Blunden, M. (2012): Geopolitics of the Northern Sea Route. *International affairs,* Vol. 88, January 2012, pp. 114-129

Bureau Veritas (2010): *Ice characteristics and ice/structure interactions, Guidance note NI 565 DT R00 E*, Bureau Veritas, 2010

Chen, Y. K., Tunik, A. L., Chen, P.Y. (1990): *Global ice forces and ship response to ice – Analysis of ice ramming forces*, Report no. SSC-342, American Bureau of Shipping, 1990, 106 pp.

Croasdale, K. R., Frederking, R. (1986): *Field techniques for ice force measurements.* Proceedings of IAHR Ice Symposium 1986, IAHR, Iowa City, Iowa, 1986, pp. 443-448.

Daley, C., Riska, K. (1995): *Conceptual framework for an ice load model*, National Energy Board, Calgary, Alberta, Canada, 1995

DNV (2009): *Ice Load Monitoring – Final Report, Report nr. 2009-0033*, Det Norske Veritas, Oslo, Norway, 2009

DNV (2011): *Rules for classification of Ships / High Speed, Light Craft and Naval Surface Craft*, Part 6 Chapter 8, Det Norske Veritas, Høvik, Norway, 2011, 18 pp.

DNV (2012): *Rules for classification of ships Part 5 Chapter 1*, Det Norske Veritas, Oslo, Norway, 2012

Fredriksen, Ø. (2012): *Ice-induced loading on ship hull during ramming*, M.Sc. Thesis, Norwegian University of Science and Technology, Faculty of Engineering Science and Technology, Department of Marine Technology, Trondheim, Norway, 2012, 70 pp.

IACS (2009): *IACS Guideline for rule development – Ship structure*, International Association of Classification Societies, 2009

IACS (2010): *Requirements concerning Polar Class*, International Association of Classification Societies, 2010

IMO (2011): *Generic guidelines for developing IMO goal-based standards*, International Maritime Organization, 2011

IPCC (2007): *Climate Change 2007 (AR4): Synthesis Report*, Intergovernmental Panel on Climate Change, IPCC, Geneva, Switzerland, pp. 104

Jansson, C-E (2011): *Lecture notes for MMA145 Ship Motions and Wave Induced Loads*, Department of Shipping and Marine Technology, Chalmers University of Technology, Göteborg, Sweden, 2011

Johnston, M., Timco, G., Frederking, R. and Miles, M. (2001): *Whole-ship motions of USCGC Healy as applied to global ice impact forces*, Proceedings 16th Internationcal Conference on Port and Ocean Engineering under Arctic Conditions, POAC'01, Ottawa, Canada, 2001, pp. 955-964)

Johnston, M., Frederking, R., Timco, G.W. and Miles, M. (2003): *MOTAN: A novel approach for determing ice-induced global loads on ships*, Proceedings MARI-TECH 2003, Montreal, Canada, 2003, 17 pp.

Johnston, M., Frederking, R., Timco, G. and Miles, M. (2004): *Using motan to measure global accelerations of the CCGS Terry Fox during Bergy bit trials*, Proceedings of OMAE04, Vancouver, Canada, 2004, 8 pp.

Jordaan, I., J. (2001): Mechanics of ice-structure interaction, Engineering Fracture Mechanics, Vol 68, 2001, pp. 1923-1960

Kongsberg (2006): *Seatex MRU, User´s Manual*, Kongsberg Seatex AS, Trondheim, Norway, 2006

Krupina, N., Likhomanov, V.A., Chernov, A.V., Gudoshnikov, Y.P. (2009): *Full-scale ice impact study of icebreaker Kapitan Nikolaev: General Description*, Proceedings of the 19th International Offshore and Polar Engineering Conference, Osaka, Japan, 2009, pp. 614-620

Likhomanov, V.A., Krupina, N.A., Chernov, A.V., Gudoshnikov, Y.P. (2009): *Results of the global ice load during in-situ research on impact of the icebreaker "Kapitan Nikolaev" on various ice formations*, Proceedings of the 19th International Offshore and Polar Engineering Conference, Osaka, Japan, 2009, pp. 593-619

Liu, Z. (2011): *Analytical and numerical analysis of iceberg collisions with ship structures*, Ph.D. Thesis, Faculty of engineering science and technology, Department of Marine technology, Norwegian University of Science and Technology, Trondheim, Norway, 2011

Lundhaug, M. (2002): *Sea Ice Studies in the Northern Sea Route by use of Synthetic Aperture Radar*, Ph.D. Thesis, Norwegian University of Science and Technology, Faculty of Natural Sciences and Technology Trondheim, Norway, 2002

MathWorks (2011): *MATLAB Version (R2011b)*, MathWorks Inc, Natick, MA, United States, Release date; 1 September, 2011.

Mejlander-Larsen, M., Nyseth, H. (2007): *Ice load monitoring*, Design and Construction of Vessels Operating in Low Temperature Environmnet, Royal Institution of Naval Architects, London, United Kingdom, 2007

Miles, M.D. (1986): *Measurement of six degree of freedom model motions using strapdown accelerometers*, Proceedings of the 21st American Towing Tank Conference, Washington D. C., 1986, 8 pp.

Nasa (2012): http://www.nasa.gov/topics/earth/features/2012-seaicemin.html, [Accessed 2013-03-13]

Nyseth, H. (2012): *Notes from data collection*, Det Norske Veritas, Oslo, Norway, 2012

Nyseth, H., Frederking, R., Sand, B., (2013): *Evaluation of global ice load impacts based on real-time monitoring of ship motions*, Proceedings of the 22nd International conference on Port and Ocean Engineering under Arctic Conditions, POAC'13, Espoo, Finland, 2013, (in press)

Pettersen (2012): http://barentsobserver.com/en/arctic/2012/11/46-vessels-through-northern-sea-route-23-11, [Accessed 2013-03-13]

Popov, Y., N. (1967): *Strength of ship sailing in ice*, Sudostroyeniye Publishing house, Leningrad, USSR, 1967, Translated by: U.S. Army Foreign Science and Technology Center, 1969

Santos-Pedro, V.M., Timco, G. W. (2001): *Canadian involvement in the USCGC Healy ice trials*, Proceedings 16th International Conference on Port and Ocean Engineering under Arctic Conditions, POAC'01, Ottawa, Canada, 2001, pp. 921-933

Suyuthi, A., Leira, B.J., Riska, K. (2011): Full scale measurements on level ice resistance of icebreaker, *International Conference on Ocean, Offshore and Arctic Engineering OMAE2011*, 30th , June, 2011

Suyuthi, A., Leira, B.J., Riska, K. (2012): Non parametric probabilistic approach of ice load peaks on ship hulls, *International Conference on Ocean, Offshore and Arctic Engineering OMAE2012*, 31st, July, 2012

Timco, G.W., Weeks, W.F. (2010): A review of the engineering properties of sea ice, *Cold Region Science and Technology*, Vol. 60, 2010, pp. 107-129.

USARC (2012): *Oil spill in Arctic waters*, United States Arctic Research Commission, Nov, 2012, 30 pp.

USGS (2008): http://www.usgs.gov/newsroom/article.asp?ID=1980, [Accessed 2013-03-13]

Verny, J., Grigentin, C. (2009): Container shipping on the Nothern Sea Route. *Int. J. Production Economics*, Vol. 122, 2009, pp. 107-117

Lewis, E., V. (1988): *"Chapter VII - Vibration". Principles of Naval Architecture: Resistance, Propulsion and Vibration, Volume II, Second Revision.* The Society of Naval Architects and Marine Engineers, 1988

WMO (2004): *WMO Sea-ice nomenclature Volume I – Terminology and codes*, World Meteorological Organization, WMO No. 259, 2004

Zou, B. (1996): *Ships in ice: The interaction process and principles of design*, Ph.D. Thesis, Faculty of engineering and applied science, Memorial University of Newfoundland, St. John`s, Canada, 1996

Appendix A – Results from developed model

Table A.1 Displacements at impact.

Event	Surge [m]	Sway [m]	Heave [m]	Roll [rad]	Pitch [rad]	Yaw [rad]
1	0.38	10.56	0.20	-	-0.003	-0.515
2	-2.57	-46.44	-0.10	-	-0.001	2.226
3	-2.18	-40.56	0.06	-	-0.002	1.981
4	-1.70	-37.29	-0.02	-	0.006	1.829

Table A.2 Velocities at impact.

Event	Surge [m/s]	Sway [m/s]	Heave [m/s]	Roll [rad/s]	Pitch [rad/s]	Yaw [rad/s]
1	-0.19	-0.09	0.21	-	-0.012	0.002
2	-0.10	0.18	0.12	-	-0.005	-0.008
3	-0.10	0.06	0.08	-	-0.003	-0.002
4	0.04	0.18	-0.14	-	0.000	-0.007

Table A.3 Accelerations at impact.

Event	Surge [m/s^2]	Sway [m/s^2]	Heave [m/s^2]	Roll [rad/s^2]	Pitch [rad/s^2]	Yaw [rad/s^2]
1	-0.30	-0.10	0.32	-0.001	-0.011	0.002
2	-0.22	0.94	0.27	0.000	-0.012	-0.014
3	-0.19	0.36	0.18	0.001	-0.004	-0.008
4	-0.15	0.11	0.10	0.004	-0.006	-0.001

Table A.4 Force components from displacements.

Event	F_surge [MN]	F_sway [MN]	F_heave [MN]	F_roll [MN]	F_pitch [MNm]	F_yaw [MNm]
1	0	0	2.75	-	-11.52	0
2	0	0	-1.59	-	-14.07	0
3	0	0	0.82	-	-9.85	0
4	0	0	0.15	-	50.65	0

Table A.5 Force component from velocity.

Event	F_surge [MN]	F_sway [MN]	F_heave [MN]	F_roll [MN]	F_pitch [MNm]	F_yaw [MNm]
1	-0.12	-0.06	-1.59	-	-15.15	-1.43
2	-0.06	0.20	-0.65	-	-7.68	2.16
3	-0.04	0.05	-0.42	-	-5.01	0.87
4	0.05	0.17	-0.01	-	6.27	2.38

Table 6 Force component from acceleration.

Event	F_surge [MN]	F_sway [MN]	F_heave [MN]	F_roll [MNm]	F_pitch [MNm]	F_yaw [MNm]
1	-2.53	-1.00	7.17	0.62	-174.94	19.67
2	-2.04	9.67	5.59	-13.28	-197.55	-158.45
3	-1.44	3.72	4.29	-4.87	-62.40	-87.85
4	-1.29	1.10	1.78	1.45	-105.58	-10.49

Table A.7 Force components in COG.

Event	F_surge [MN]	F_sway [MN]	F_heave [MN]	F_roll [MNm]	F_pitch [MNm]	F_yaw [MNm]
1	-2.65	-1.06	8.34	0.62	-175.55	19.64
2	-2.10	9.87	3.36	-13.28	-198.05	-158.40
3	-1.48	3.77	4.69	-4.87	-62.74	-87.83
4	-1.24	1.27	1.92	1.45	-104.27	-10.43

Table A.8 Resulting force in COG and POI.

Event	F_poi [MN]	F_cog [MN]
1	5.34	8.81
2	6.51	10.63
3	3.04	6.19
4	1.68	2.62

Appendix B – Results from similar studies

Table B.1 Names of ships subject for study in the MOTAN project and some design parameters.

Ship name	Loa (m)	Breath (m)	Draft (m)	Displacement (tons)
CCGS Louis S. St. Lourent	119,8	24,38	9,91	15324
USCGS Healy	130	25	8,92	16257

CCGS Louis S. St. Lourent

Table B.2 Maximum motion response during trials with CCGS Louis S. St. Lourent, Johnston et al. (2001).

Motion	Maximum amplitude	Ice type
Heave	1.0 m	Multi-year ice
Sway	1.5 m	Ridged multi-year ice
Surge	1.9 m	Multi-year ice
Roll	7.6°	Ridged multi-year ice
Pitch	1.8°	Multi-year ice
Yaw	1.5°	Multi-year ice
Heave acceleration	1.1 m/s²	Ridged multi-year ice
Sway acceleration	1.9 m/s²	Ridged multi-year ice
Surge acceleration	1.0 m/s²	Multi-year ice
Roll acceleration	2.8 °/s²	Ridged multi-year ice
Pitch acceleration	1.8 °/s²	Ridged multi-year ice
Yaw acceleration	1.5 °/s²	Multi-year ice

Table B.3 Global force computation for CCGS S. St. Lourent, Johnston et al. (2003).

Force (MN)	Speed (kts)	Ice type
10.4	10.5	First-year ice
12	10.3	First-year ice
12.4	10	First-year ice
9.5	5.6	Multi-year ice
17.3	5.3	Multi-year ice
11	4.9	Multi-year ice
15.7	4.5	Multi-year ice
16.7	4	Multi-year ice
12	3	Multi-year ice
13	2	Multi-year ice
12	1.2	Multi-year ice
13.7	9	Second-year ice
14	9	Second-year ice
10	9	Second-year ice
9.5	8.4	Multi-year ice
12	7.8	Multi-year ice
10	6.3	Multi-year ice
12.6	6.1	Multi-year ice
9	6.5	Multi-year ice
12.5	4.5	Multi-year ice
5.7	2.3	Multi-year ice

USCGC Healy

Table B.4 Forces on USCGC Healy, Johnston et al. (2001).

Force (MN)	Type of force	Ice type	Maximum pitch angle (°)	Maximum roll angle(°)
4,3 MN	Vertical Bow force	First-year ridge	0,7	4,9
3,8 MN	Vertical Bow force	First-year ridge	0,4	-